

**STUDY OF THE MECHANICAL PROPERTIES OF ELECTROPLATED Zn-Ni
ALLOY COATING**

MD. MONIRUZZAMAN

A thesis submitted to the Department of Metallurgical Engineering Bangladesh University of Engineering and Technology, Dhaka, in partial fulfillment of the requirements for the degree of Master of Science in Engineering (Metallurgical)



August, 1995


**BANGLADESH UNIVERSITY OF ENGINEERING AND TECHNOLOGY
DHAKA, BANGLADESH.**



DECLARATION

This is to certify that this research work has been carried out by the author under the supervision of Dr. A.S.M.A. Haseeb, Assistant Professor, Department of Metallurgical Engineering, BUET, Dhaka, and it has not been submitted elsewhere for the award of any other degree or diploma.


Countersigned

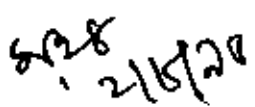

02/08/95
Supervisor


Moniruzzaman

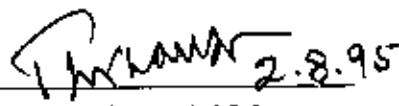
Signature of the Author

The undersigned examiners appointed by the Committee of Advanced Studies and Research (CASR) hereby recommend to the Department of Metallurgical Engineering, Bangladesh University of Engineering and Technology, Dhaka, the acceptance of the thesis entitled **"STUDY OF THE MECHANICAL PROPERTIES OF ELECTROPLATED Zn-Ni ALLOY COATING"** submitted by Md. Moniruzzaman, B.Sc. Engg. (Metallurgical) in partial fulfillment of the requirements for the Degree of Master of Science in Engineering (Metallurgical).

1.  2/8/95

Dr. A.S.M.A. Haseeb
Assistant Professor
Department of Metallurgical Engg.
BUET, Dhaka. Chairman
(Supervisor)
2.  2/8/95

Head
Department of Metallurgical Engg.
BUET, Dhaka. Member
(Ex-officio)
3. 

Dr. A.S.W. Kurny
Professor
Department of Metallurgical Engg.
BUET, Dhaka. Member
4.  2.8.95

Professor Md. Serajul Islam
256/2A, Sultangonj
Rayer Bazar, Dhaka. Member
(External)

ACKNOWLEDGEMENT

The author is deeply indebted and much obliged to Dr. A.S.M.A. Haseeb, Assistant Professor, Department of Metallurgical Engineering, Bangladesh University of Engineering and Technology (BUET), Dhaka for his kind supervision and encouragement in carrying out the project work as well as in writing this thesis. His assistance through profound knowledge and experience has made the successful completion of the thesis possible.

The author is grateful to professor Md. Mohafizul Haque, Head, Department of Metallurgical Engineering, BUET, Dhaka for his kind inspiration in every step of work.

The author expresses his thanks to Mr. Md. Zahedul Huq, Assistant Professor, Department of Metallurgical Engineering, BUET and to all research students working under the supervision of Dr. A.S.M.A. Haseeb for their kind help and suggestions.

Thanks are also due to the officers and staff of the Department for their help in various stages of the study.

**Department of Metallurgical Engineering
BUET, Dhaka.**

The Author

ABSTRACT

Electrodeposition of Zn-Ni alloy coatings was carried out in three different sulphate baths. Uniform, adherent coatings were obtained at room temperature in the pH range of 1.8-3. Chemical analysis showed that the three baths yielded Zn-Ni alloy coatings with 7%, 14.4% and 40% nickel. The coatings were examined for their mechanical properties viz., microhardness, wear resistance and ductility. X-ray diffraction experiments were carried out to find out the phases present in the coatings. Pure zinc coatings were also deposited and tested for comparison.

X-ray diffraction study showed that coatings with 40% and 14.4% Ni and pure zinc were deposited with equilibrium phase structures. X-ray diffraction patterns of annealed 40% Ni and 14.4% Ni samples also showed some extra unknown peaks.

The microhardness was found to increase with nickel content of the deposit. As-deposited coatings with 40% Ni, 14.4% Ni and 7% Ni were found to possess a hardness value of 487 VHN, 460 VHN and 390 VHN respectively while the annealed samples showed a little lower value of hardness. As-deposited pure zinc coating exhibited a hardness of 180 VHN only.

Wear behaviour of 14.4% Ni, 7% Ni and pure zinc coatings was studied under dry sliding conditions using a pin-on-disc type apparatus at a constant rpm of 500. Wear tests were carried out under three different loads viz., 250 gm, 175 gm and 120 gm. Tests were carried out for

sliding distance ranging from 416 to 1248 meter. All tests were performed in the ambient air at room temperature. Extent of wear damage was investigated by means of measurement of width of wear scar and metallography. Zn-Ni coating with 14.4% Ni was found to be more wear resistant than the coating with 7% Ni. Pure zinc coating is found to be the least resistant to wear.

It was found that ASTM B 489-68 bend test is not suitable for measurement and comparison of ductility of zinc and zinc-nickel alloys.

CONTENTS

ACKNOWLEDGEMENTS	i
ABSTRACT	ii

Contents	Page No.
1.INTRODUCTION	1
1.1 An Overview of Zn-Ni Alloy Coating	1
1.2 Present State and Objective of the Work	3
2. LITERATURE REVIEW	4
2.1 ELECTRODEPOSITION ASPECT	
2.1.1. Thermodynamics of Electrodeposition Reactions	4
2.1.2 Kinetics of Electrodeposition Reactions	6
2.1.3 General Conditions for Electrodeposition of Alloys	8
2.1.4 Role of Static Potentials in the Electrodeposition of Alloys	9
2.1.5 Methods of Bringing Static Potentials of Metals Closer Together	12
2.1.6 Principles of Alloy Deposition	14
2.1.7 Advantages and Disadvantages of Alloy Deposition	16

2.2 VARIATION IN THE COMPOSITION OF ELECTRODEPOSITED ALLOYS WITH THE COMPOSITION OF THE BATH AND THE PLATING PARAMETERS	16
2.2.1 Plating Variables	16
2.2.2 Types of Alloy Plating Systems	17
2.2.3 Effect of Metal Ratio of the Bath on the Composition of the Deposit	19
2.2.4 Effect of Total Metal Content of the Bath on the Compositions of the Deposit	22
2.2.5 Effect of pH of the Plating Bath on the Composition of the Deposit	23
2.2.6 Relation Between Current Density and Composition of Electrodeposited Alloys	25
2.2.7 Effect of Bath Temperature on Composition of Electrodeposited Alloys	27
2.2.7.1 General	27
2.2.7.2 Effect of Bath Temperature on Composition of Alloys in Anomalous Co-deposition.	28
2.2.8 Effect of Agitation of Bath or Rotation of Cathode on the Composition of Electrodeposited Alloys.	29
 2.3 PROPERTIES OF ELECTRODEPOSITED ALLOYS	 30
2.3.1 Mechanical Properties of Electrodeposited Alloys	30
2.3.1.1 Hardness	30
2.3.1.2 Ductility	32
2.3.1.3 Wear Behavior	33

2.3.2 Protective Value of Alloy Coatings	34
2.3.2.1 General Considerations	34
2.3.2.2 Advantages of Using Alloy Coatings and Examples of Corrosion-Resistant Alloy Coatings.	35
3. EXPERIMENTAL	38
3.1 Materials	38
3.2 Preparation of Specimen for Electrodeposition	38
3.3 Electrodeposition Set-Up	40
3.4 Electroplating Operation	41
3.5 Electrodeposition to Constant Thickness	42
3.6 Method of Investigation	43
3.6.1 Chemical Analysis of the Zn-Ni Alloy Deposit	44
3.6.2 Wear Test	44
3.6.3 Microhardness Measurement	45
3.6.4 Phase Study Through X-ray Metallography	46
3.6.5 Ductility Test	46
4. RESULTS AND DISCUSSIONS	48
4.1 Electrodeposition of Zn-Ni Alloy Coatings	48
4.2 X-ray Investigation	50
4.3 Microhardness Measurements	56
4.4 Wear Test Evaluation	58
4.5 Ductility Test	70
5. CONCLUSIONS	71
5.1 Conclusions Drawn from the Present Work	71

5.2 Suggestions for Further Work	72
6. REFERENCES	73
7. APPENDIX: A	78

CHAPTER: ONE

1. INTRODUCTION

1.1 An Overview of Zn-Ni Alloy Coating

In response to a strong demand for improvement in the corrosion resistance of coated steel particularly for automotive applications, Zn-electroplating technology has made great progress since the late 1970s, both in quality performance and its manufacturing process. That is, the quality performance of coated products were enhanced by the development of alloy electroplated steel, including Zn-Co, Zn-Ni, Zn-Fe alloy electroplated steel and others. A Zn-Co alloy containing a small amount of alloying elements [1] was the first found to be corrosion-resistant and thus attracted strong attention in the field of Zn-alloy electroplating. The alloy exhibited between 2 and 6 times the corrosion resistance of pure Zn in a salt-spray test. Subsequently, Zn-Ni alloy electroplating was developed. Although this had been investigated for a long time [2], it was the latter half of the 1970s when electroplating of Zn-Ni alloy began to be applied to continuous steel strip [3]. They attain a higher corrosion resistance than the Zn-Co alloys, that is, 4 to 8 times the corrosion resistance of pure Zn, in accordance with a higher concentration of alloying element. In addition to excellent corrosion resistance, Zn-Ni alloys are the most easily manufactured of Zn-alloy coatings. Consequently, the potential economic advantages in using Zn-Ni in stead of Zn-coating on steel have been recognized and Zn-Ni electroplated steel became a representative product in the field.

Since the advent of steel-belted radial tires, brass-coated steel cord is the material most widely used for the reinforcement of automobile tires [4]. While the conventional brass coating offers several advantages, it also suffers from two major deficiencies resulting from the electrochemical characteristics of brass-steel couple under salt corrosion and humidity aging [5,6]. Cuts in the tire tread surface may be produced in service. Deep cuts in the tread down to the steel cords expose the latter to corrosion through the formation of oxygen concentration cells [6].

At oxygen-depleted acidic (low pH) regions deeper in the cut, the brass coating is cathodic to steel; hence it accelerates the corrosion of the underlying steel, thus reducing the strength of reinforcing steel cords. Under conditions existing at oxygen-rich (high pH) regions near the surface of the exposed cord, the brass coating itself corrodes through dezincification followed by dissolution of brass. This, in turn, results in the deterioration of the adhesion between brass coating and vulcanized natural rubber (NR) compound. Further, the fully deformed brass coating on the final cord filaments is porous and does not offer a barrier protection to the steel core.

A copper-free alloy coating system based on Zn-Ni and Zn-Co binary alloys that can overcome the drawbacks of conventional brass coatings was conceived by Van Ooij [7]. The coating would consist of a zinc-rich first alloy layer on steel to provide galvanic protection against corrosion, followed by a nickel-rich second alloy layer for improved initial and aged adhesion to NR compounds. The dual-layer coating design offers sacrificial protection (Zn-rich layer), barrier protection (Ni-rich layer) and better overall formability. Because of the cathodic nature of nickel-rich surface layer, it is reasonable to expect excellent phosphatability and paintability as well. Thus the coating system offers significant advantage in automotive applications.

1.2 Present State and Objective of the Work

has been Zn-Ni coated steel sheet can be used on automobile bodies, C.I. sheets, steel cord of automobile tires and other applications requiring corrosion resistance. For such type of applications, the Zn-Ni alloy coating should also have adequate mechanical properties e.g. wear resistance, micro-hardness, ductility, decorative properties etc. Information available in the literature on the effect of composition and structure of the Zn-Ni coating on its mechanical properties is meager. It is, therefore, the objective of the present work to investigate systematically the effect of composition and structure of Zn-Ni alloy coating on its mechanical properties. The effects are followed by wear test, micro-hardness measurement, X-ray metallography and chemical analysis. Microhardness and metallography tests are also performed for heat-treated Zn-Ni alloy coating and a comparison of the results thus obtained attempted.

 CHAPTER: TWO

2. LITERATURE REVIEW

2.1 ELECTRODEPOSITION ASPECT

2.1.1 Thermodynamics of Electro-deposition Reactions

In an electrodeposition cell, a reaction of the type



can take place at the cathode. The metal electrode consists of metal ions in a crystal structure. The transfer of a metal ion from the electrolyte structure to the metal structure will be accompanied by a free energy change ΔG . Thermodynamics tells that in a system with only PV work, the free energy changes for the transport of n moles of matter i from phase 1 to phase 2 according to

$$dG = VdP - SdT + \mu^2_i dn - \mu^1_i dn \quad \dots\dots\dots(2.2)$$

where μ^1_i and μ^2_i are the chemical potentials in phase 1 and 2 respectively. In an electrochemical system, not only PV-work, but also electrical work — the work accompanying the transport of electrical charge over a potential difference — must be taken into account. Equation (2-2) then transforms into

$$dG = VdP - SdT + (\mu_2^i - \mu_1^i)dn + (\phi_2^i - \phi_1^i)zFdn \dots(2-3)$$

where $zF(\phi_2^i - \phi_1^i)$ is the electrical work involved in the transport of the electrical charge of 1 mol of ions from phase 1 to phase 2, ϕ is the electrical potential and F is Faraday's constant. The equilibrium criterion, with P and T constant, is that the free energy is minimum, thus $dG=0$ and consequently $\mu_1^i = \mu_2^i$. So the condition for equilibrium is now [from (2-3)]

$$\mu_1^i + zF\phi_1^i = \mu_2^i + zF\phi_2^i$$

$$\mu_1^{\text{El.1}} = \mu_2^{\text{El.2}}$$

For the electrochemical reaction, [Eq.(2-1)], taking place at the electrode:

$$\Delta\phi_e = \phi_M - \phi_S \text{ [where } \Delta\phi_e = \text{Potential difference between the metal at the electrode and its ions in solution] and}$$

$$\Delta G^{\text{El}} = \Delta G^{\circ} - RT \ln a_{M^{z+}} + zFA\phi_e \dots\dots\dots (2-4)$$

where ΔG° = Standard free energy of reaction (2-1)

$$a_{M^{z+}} = \text{Activity of } M^{z+}$$

Under standard conditions ($a_{M^{z+}} = 1$) at equilibrium,

$$\Delta G^{\text{El}} = 0 \text{ and } \Delta\phi_e = \Delta\phi_e^{\circ}$$

Hence (2-4) transforms to

$$0 = \Delta G^{\circ} - 0 + zFA\phi_e^{\circ}$$

$$\Rightarrow \Delta G_0 = -zF\Delta\phi_e^0 \quad \dots\dots\dots(2-5)$$

where, $\Delta\phi_e^0$ = Standard electrode potential.

Combination of Eqs. (2-4) and (2-5) leads to

$$0 = -zF\Delta\phi_e^0 - RT\ln a_{M^{z+}} + zF\Delta\phi_e$$

$$\Rightarrow \Delta\phi_e = \Delta\phi_e^0 + (RT/zF) \ln a_{M^{z+}} \quad \dots\dots\dots(2-6)$$

Equation (2-6), known as Nernst equation, gives the effect of concentration on electrode potential.

2.1.2 Kinetics of Electrodeposition Reactions

From the moment that a current flows through an electrode, the electrode acquires a potential different from the reversible equilibrium potential. It is well to note here that equilibrium means dynamic equilibrium and that although no net current flows through the electrode, oxidation and reduction reactions will take place simultaneously, such that the oxidation current density i_{ox} is equal in magnitude to the reduction current density i_{red} . Both are, at equilibrium, equal to the so-called exchange current density and the equilibrium potential across the electrode is $\Delta\phi_e$.

In order to realize electrodeposition at a cathode, a net current $i = (i_{ox} - i_{red}) < 0$ has to flow through the cathode. Therefore the potential $\Delta\phi$ over the electrode interface has to deviate from $\Delta\phi_e$. This deviation is called the activation overpotential (η).

$$\text{Hence } \Delta\phi = \Delta\phi_e + \eta$$

The term 'activation' refers to the fact that the electrode reaction is a kinetic process, in which substances must acquire a certain activation energy before they can jump through the electrode interface. Deviation from the equilibrium potential is called polarization.

As a result of the electrode reaction, the ionic concentration tends to change in the vicinity of the electrode, resulting in a concentration overpotential η_{con} . For a reduction reaction at the cathode, for example, the concentration of positive ions is lowered, and the equilibrium potential shifts according to the Nernst equation. If, as a result of an increasing cathodic polarization, the reduction current density is increased, positive ions have to be brought to the cathode surface faster and faster. This can occur by

- i) migration under influence of the electrical field
- ii) diffusion due to the created concentration differences
- iii) natural or forced convection.

Another component is the crystallization overpotential (η_{cr}) originating from difficulties encountered with nucleation and growth. Minute concentrations of foreign substances can drastically increase the crystallization overpotential, and thus effectively slow down the electrodeposition process. The global electrode overpotential is, now

$$\eta_{\text{tot}} = \eta + \eta_{\text{con}} + \eta_{\text{cr}} \quad \text{-----(2-7)}$$

An electrodeposition cell contains two electrodes: a cathode and an anode. Both contribute to the total cell potential according to equation (2-7).

In addition there is the resistance of the electrolyte leading to a potential IR , and various other resistances in the cell circuit creating a potential E_R . The total cell potential is then

$$E_{\text{tot}} = E_{\text{rev}} + \eta_{\text{tot}}^{\text{an}} + \eta_{\text{tot}}^{\text{cat}} + IR + E_{\text{R}}$$

The practical cell potential is therefore sometimes much higher than the reversible cell potential calculated from purely thermodynamic considerations.

2.1.3 General Conditions for Electrodepositing Alloys

Superficially, the procedure for depositing an alloy differs in no important respect from that for depositing a single metal — a current is passed from electrodes through a solution and a metal deposits upon the cathode. However, the problem of finding conditions for depositing a given alloy in the form of a sound, strong, homogeneous coating is not as easily solved as for a single metal. The simultaneous deposition of two or more metals without regard to the physical nature of the deposit is a relatively simple matter, for it is necessary only to electrolyze a bath of the mixed metallic salts at a sufficiently high current density. Unfortunately, the deposits so obtained are usually loose, spongy, non-adherent masses, contaminated with basic inclusions, and are not the type of deposit of interest. Thus, the use of a high current density is not a means of solving the problem of alloy deposition.

A preliminary and rather obvious requirement for codepositing two or more metals from aqueous solution is that at least one of the metals be individually capable of being deposited from aqueous solution. The most important practical consideration involved in the codeposition of two metals is that their deposition potentials be fairly close together. The importance of this consideration follows from the well-known fact that the more noble metal deposits preferentially, frequently to the complete exclusion of the less noble metal. To simultaneously codeposit the two metals, conditions must be such that the more negative potential of the less noble metal can be attained without employing an excessive current density. Hence, the need for having the potentials of the two metals close together.

2.1.4 Role of Static Potentials in the Electrodeposition of Alloys

The table of standard electrode potentials, Table 2.1 may serve as a rough but not too reliable guide for deciding if two metals may be co-deposited from a simple salt solution. The data in Table 2.1 apply only to very specific conditions and are, therefore, of limited applicability. This must be further emphasized before proceeding with a discussion of their value for predicting the probability of co-deposition of two metals. The electrode potentials in Table 2.1 apply only to the equilibrium potentials of the metals in a solution of their simplest ions and are just about the most positive (most noble) potentials at which the metals can be deposited. In actual deposition, because of polarization, the deposition potentials are more negative than the standard potentials.

The deduction from a table of electrode potentials of the probability of, and the conditions for, depositing a single metal is not straightforward. As an example, if one were to make a naïve interpretation of Table 2.1 without regard to practical considerations, one would come to the conclusion that metals with electrode potentials more negative than hydrogen could not be deposited from aqueous solution because hydrogen would deposit at a more positive (more noble) potential. Actually, hydrogen deposits at a much more negative potential than its equilibrium value on many kinds of metal electrodes (the phenomenon of hydrogen overvoltage), and, consequently, the potentials of some of these metals can be attained in aqueous solution without excessive discharge of hydrogen. Even manganese with an equilibrium potential of -1.18 V can be deposited from aqueous solution by virtue of its hydrogen overvoltage. The existence of this phenomenon is fortunate for electrodepositions, because the majority of the metals in which electroplaters are interested have potentials less noble than that of hydrogen. Another example of the opposite kind concerns the metals vanadium, molybdenum, germanium and tungsten which have the following electrode potentials, respectively: -0.253 , -0.2 , -0.15 and -0.09 volt. According to Table 2.1, these

Table 2.1
Standard Electrode Potentials (E^0)

Electrode Reaction	E^0 (Volts), 25 ⁰ C
$\text{Na} = \text{Na}^+ + e$	-2.712
$\text{Mg} = \text{Mg}^{+2} + 2e$	-2.340
$\text{Al} = \text{Al}^{+3} + 3e$	-1.670
$\text{Mn} = \text{Mn}^{+2} + 2e$	-1.180
$\text{Zn} = \text{Zn}^{+2} + 2e$	-0.762
$\text{Co} = \text{Co}^{+2} + 2e$	-0.277
$\text{V} = \text{V}^{+2} + 2e$	-0.253
$\text{Ni} = \text{Ni}^{+2} + 2e$	-0.250
$\text{Mo} = \text{Mo}^{+3} + 3e$	-0.200
$\text{Ge} = \text{Ge}^{+4} + 4e$	-0.150
$\text{Sn} = \text{Sn}^{+2} + 2e$	-0.136
$\text{Pb} = \text{Pb}^{+2} + 2e$	-0.126
$\text{W} = \text{W}^{+6} + 6e$	-0.090
$\text{H}_2 = 2\text{H}^+ + 2e$	0.000
$\text{Bi} = \text{Bi}^{+3} + 3e$	+0.320
$\text{Cu} = \text{Cu}^{+2} + 2e$	+0.345
$\text{Cu} = \text{Cu}^+ + e$	+0.522
$\text{Ag} = \text{Ag}^+ + e$	+0.800
$\text{Pt} = \text{Pt}^{+2} + 2e$	+1.200
$\text{Au} = \text{Au}^{+3} + 3e$	+1.420
$\text{Au} = \text{Au}^+ + e$	+1.620

metals ought to be more readily depositable from aqueous solution than cobalt with a potential of -0.277 volt. However, none of these metals have been deposited from aqueous solution in the pure state, whereas cobalt is readily deposited. We do not know why these metals do not deposit but the situation is not unique. The nonoccurrence of reactions which are thermodynamically possible is quite common in chemistry. This means that other requirements must be satisfied as well as the energetics of the process.

To sum up the discussion of electrode potentials, we see, on one hand, that many metals can be deposited, which would not be expected to deposit on the basis of equilibrium potentials; and on the other hand, that metals which are theoretically capable of being deposited have not been deposited from aqueous solution.

Despite these inconsistencies, the table of electrode potential can be utilized to derive some conclusions regarding alloy deposition from acid solutions of simple ions. Metals which are close together in table 2.1 should in general be more readily codeposited than metals which are widely separated. As a rough guide, reasonably satisfactory co-deposition will occur if the static potentials of the metals are not over 0.2 volt apart. However, exceptions may be noted; for example, Zn and Ni may be co-deposited from a simple salt bath, although their electrode potentials are about 0.5 volt apart. An exception of the opposite kind occurs with some of the noble metals. For example, silver and palladium do not readily co-deposit to yield good alloys although their potentials are very close together. This discussion shows that the predictions concerning alloy deposition from electrode potentials alone are not wholly reliable and may be misleading because many unpredictable specific effects occur with each pair of metals.

2.1.5 Methods of Bringing Static Potentials of Metals Closer Together

The potential of metal dipping into a solution of its ions at unit activity is the standard electrode potential of the metal, E^0 . When the activity of the ions is not unity the static potential E_s is given by

$$E_s = E^0 - (RT/nF) \ln a \quad \dots\dots\dots(2-8)$$

where, R = Gas constant

T = Absolute temperature

n = Valence change in the reaction metal-metal ion

F = The Faraday's constant

a = Activity of metal ion

Equation (2-8) represents the equilibrium reversible conditions. Irreversible factors (concentration, polarization, overvoltage etc.) however enter in if current is passed so that metal deposits from a solution. The actual deposition potential is then given by

$$E_D = E_s + P$$

Where P is a measure of irreversible effects, i.e. the additional potential that has to be provided to keep the reaction going at the required speed.

To codeposit two metals, the deposit potential of the two metals should be nearly equal. The following conditions should, therefore, be satisfied for co-deposition of alloys:

$$E_D' = E_D''$$

$$\Rightarrow E_{s'} + P' = E_{s''} + P''$$

$$\Rightarrow E^{O'} - (RT/n'F)\ln a' + P' = E^{O''} - (RT/n''F)\ln a'' + P'' \dots (2-9)$$

where $E_{D'}$, $E^{O'}$ and a' are deposition potential, electrode potential and activity of one metal respectively. Similarly $E_{D''}$, $E^{O''}$ and a'' are deposition potential, electrode potential and activity of the other metal respectively desired to be co-deposited. In equation (2-9), R and F are fixed. T is constant in any given case. Thus, equation (2-9) can be satisfied only in the following ways:

i) Metals placed close together in electro-chemical series: If the two metals to be co-deposited are already close together in the electro-chemical series, $E^{O'}$ may become equal to $E^{O''}$. A good example is Sn-Pb alloy.

$$E^O \text{ for Sn} = -0.14V \quad E^O \text{ for Pb} = -0.13V$$

These are so close together that Sn and Pb may be co-deposited from solutions of their simple salts with no difficulty. Generally metals whose E^O values differ by less than 0.2 V can be co-deposited from simple salt solutions because polarization may bring the potential values closer together.

ii) Adjustment of $a_{O'}$ and $a_{O''}$. If $E^{O'}$ does not equal $E^{O''}$ the activity $a_{O'}$ and $a_{O''}$ must be adjusted to make the deposition potentials equal

The Nernst equation $[E = E^O + (0.059/n) \log a_{M^{n+}}]$ relates electrode potential to metal ion activity and consideration of this equation shows that a reduction in ion activity corresponds to a potential shift in the negative direction and conversely an increase in ion activity moves the

potential to more positive values. For a monovalent ion the shift is 0.059 V per order of magnitude change in activity. A well-known means of reducing the ion activity of the more noble metal is the addition of complexing agents. As an example let us consider the alloy deposition of Ag-Pb alloys.

The E^0 values are : Ag = + 0.789, Pb = 0.13

The potentials may be equalized if the more noble metal is complexed (Ag) and the less noble metal maintained uncomplexed. Only Ag forms a cyanide complex and from the Nernst equation we can calculate the activity of Ag ions required to lower the potentials to -0.13 V.

$$-0.13 = + 0.789 + 0.059 \log [Ag^+]$$

$$\Rightarrow [Ag^+] = 10^{-16} M.$$

This can be achieved by cyanide complexing provided an excess of cyanide ion is maintained

The most common complexants are cyanide, halide and amphoteric oxides like stannate, but amines, citrates, tartarets, etc. find application

2.1.6 Principles of Alloy Deposition

The six principles of alloy deposition are:

- i) If an alloy plating bath, which is in continuous operation, is replenished with two metals in a constant ratio, M/N (for example, by adding metallic salts or by the use of soluble anodes), the ratio of the metals in the deposit will approach and ultimately take on the value M/N .

ii) An increase in the metal-percentage (or ratio) of a parent metal in an alloy plating bath results in an increase in its percentage (or ratio) in the deposit.

iii) In alloy deposition, the ratio of the concentration of the more readily depositable metal to the other is smaller at the cathode-solution interface than in the body of the bath.

iv) In the deposition of alloys from the normal alloy plating systems, the most fundamental mechanism is the tendency of the concentrations of the metal ions at the cathode-solution interface to approach mutual equilibrium with respect to the two parent metals. Both principles ii) and iv) lead to the relation:

$$C_m / C_n < C_m^0 / C_n^0$$

Where, C_m = Concentration of more readily depositable metal at the cathode-solution interface.

C_n = Concentration of less readily depositable metal at the cathode-solution interface.

C_m^0 = Concentration of more readily depositable metal in the body of the bath.

C_n^0 = Concentration of less readily depositable metal in the body of the bath

v) A variation in a plating condition that brings closer together the potentials for the deposition of the parent metals separately — that is, decreases the interval of potential between them increases the percentage of the less noble metal in the electrodeposited alloy and vice-versa.

vi) In depositing alloys in which the content of the less noble metal increases with current density, the operating conditions for obtaining the more constant composition of deposit are :

(a) constant potential if the uncontrollable variable affect the potentials of the more noble metal and (b) constant current density if the uncontrollable variables affect the potentials of the less

noble metal. Conditions (a) and (b) are interchanged if the content of the less noble metal decreases with current density.

2.1.7 Advantage and Disadvantage of Alloy Deposition

Alloy deposits, offer certain advantages over single metal deposits. These are :

- i) Increased corrosion resistance due to greater density and finer grain structure,
- ii) Combination of properties of the individual constituents,
- iii) New properties, unlike the individual constituents and
- iv) Tailor-made properties by proper selection of the constituents.

The disadvantages of alloy deposition include :

- i) The greater control required,
- ii) The difficulty of reproducing the alloy composition and
- iii) The greater attention to the anode systems used and their effects on the solution constituents and complexes.

2.2 VARIATION IN THE COMPOSITION OF ELECTRODEPOSITED ALLOYS WITH THE COMPOSITION OF THE BATH AND THE PLATING PARAMETERS

2.2.1 Plating Variables

The composition of an electrodeposited alloy is a function of a large number of variables, the main ones of which are as follows :

A. Variables of bath composition

1. Concentrations of depositable metals
 - a) Ratio of the concentrations of depositable metals to each other.
 - b) Total concentration of the depositable metals

2. Concentration of complexing agents
 3. pH of plating bath
 4. Presence of addition agents
 5. Presence of indifferent electrolytes or conducting salts.
- B Variables of bath operation**
1. Current density
 2. Temperature
 3. Agitation of bath or movement of cathode
- C. Miscellaneous Variables**
1. Cathode current efficiency
 2. Shape of cathode
 3. Basis metal
 - 4 Thickness of deposit
 5. Type of current.

2.2.2 Types of Alloy Plating Systems

The data on the effects of variables on the composition of electrodeposited alloys constitute a massive array of details. The organization, presentation and theoretical discussion of these data are greatly simplified by dividing all of the alloy plating processes into five types. These are :

- i) Regular codeposition
- ii) Irregular codeposition
- iii) Equilibrium codeposition
- iv) Anomalous codeposition
- v) Induced codeposition.

Types i) -iii) are collectively referred to as normal alloy plating systems and are characterized by the preferential deposition of the more noble metal. Types iv) and v) are referred to as abnormal codeposition because the more noble metal does not necessarily deposit preferentially.

i) Regular Codeposition: Regular codeposition is characterized by the deposition being under diffusion control. The effects of plating variables on the composition of the deposit are determined by changes in the concentrations of metal ions in the cathode diffusion layer and are predictable from simple diffusion theory. The percentage of the more noble metal in the deposit is increased by those agencies that increase the metal ion content of the cathode diffusion layer. The agencies are: increase in total metal content of bath, decrease of current density, elevation of bath temperature and increased agitation of bath. Deposition of Pb-Sn, Bi-Ca etc. are the examples of regular codeposition system.

ii) Irregular Codeposition: The system is characterized by being controlled by the potentials of the metals (cathode potentials) against the solution to a greater extent than by diffusion phenomena. The effects of some of the plating variables on the composition of the deposit are in accord with simple diffusion theory and the effects of others are contrary to diffusion theory. Also, the effects of plating variables on the composition of the deposit are much smaller than with the regular alloy plating systems. Irregular codeposition is most likely to occur with solutions of complex ions. It is the least well characterized of the five types. The examples of this system are the deposition of brass, bronze and Sn-Zn.

iii) Equilibrium Codeposition: Equilibrium codeposition is characterized by deposition from a solution which is in chemical equilibrium with both of the parent metals. Only a few alloy plating systems of this type have been investigated. There are the Cu-Bi and Pb-Sn alloys deposited from an acid bath and perhaps Cu-Ni alloys deposited from a thiosulfate bath.

iv) Anomalous Codeposition: Anomalous codeposition is characterized by the anomaly that the less noble metal deposits preferentially. With a given plating bath, anomalous codeposition occurs only under certain conditions of concentration and operating variables.

Otherwise the codeposition falls under one of the three other types. Anomalous codeposition can occur in baths containing either simple or complex ions of the metals. Anomalous codeposition is rather rare. Zn-Ni alloy deposition is of this type.

v) Induced Codeposition : Induced codeposition is characterized by the deposition of alloy containing metals, such as Mo, W or Ge, which cannot be deposited alone. However, these metals readily codeposit with the iron group metals. Metals which stimulate deposition are called inducing metals and the metals which do not deposit by themselves are called reluctant metals. The effects of the plating variables on the composition of the alloys of induced codeposition are more vagarious and unpredictable than the effects on the composition of alloys of any of the other types of codeposition.

2.2.3 Effect of Metal Ratio of the Bath on the Composition of the Deposit

The relation between the composition of an electrodeposited alloy and the ratio of the parent metals in the bath is the most important relation in alloy plating system. One feature of Figs. 2.1 and 2.2 is that they contain an auxiliary line, AB, which is referred to as the 'composition reference line'. It is used as an aid visualizing the relation between the percentage composition of the alloy and the metal-percentage of the bath. Points falling upon the composition reference line would represent alloys having the same percentage composition as the metal percentage of the bath.

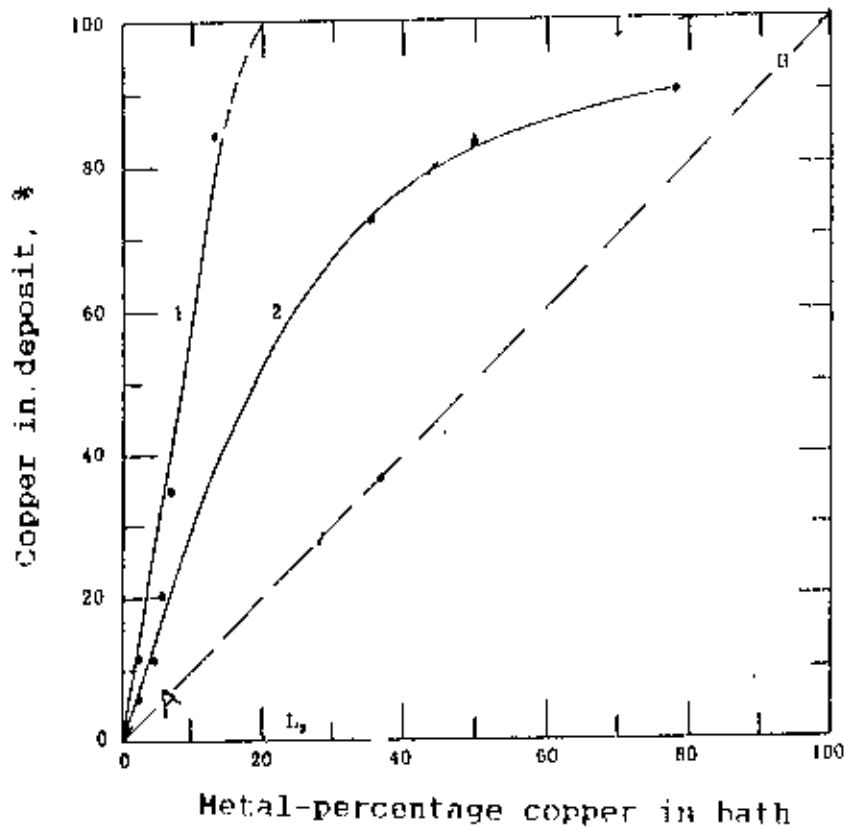


Fig.2.1: Typical curves illustrating the relation between the composition of electrodeposited alloys and the composition of the bath in normal co-deposition.

Curve 1: Bismuth-copper alloys deposited from perchlorate bath [9]

Curve 2: Copper-zinc alloys deposited from cyanide bath [10]

A composition curve that rises above the composition reference line indicates that the metal in question is preferentially deposited, because its percentage in the deposit is larger than its metal percentage in the bath. In normal codeposition, the more noble metal deposits preferentially, hence the curve for the percentage of the more noble metal in a deposit always lies above the composition reference line. Similarly, the curve representing the percentage of the less noble metal plotted against its metal percentage in the bath lies below the composition reference line.

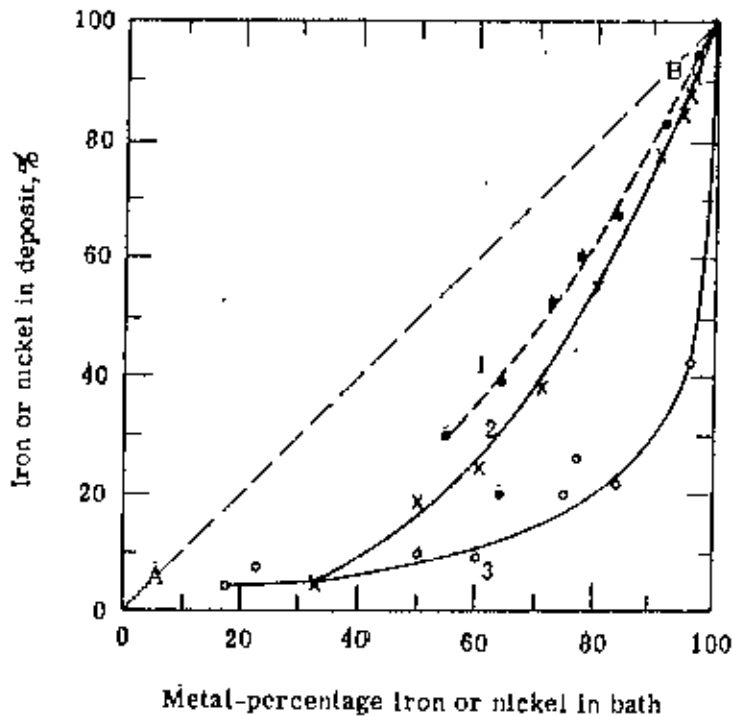


Fig.2.2: Relation between the composition of the deposit and the composition of the bath in anomalous co-deposition.

Curve 1: Iron-zinc alloys deposited from sulfate bath [11]

Curve 2: Nickel-cobalt alloys deposited from chloride bath [12]

Curve 3: Nickel-zinc alloys deposited from sulfate bath [13]

Fig. 2.2 illustrates the relation between the composition of the deposit and the composition of the bath in anomalous codeposition. Three different alloys Fe-Zn (curve 1), Ni-Zn (curve 3) and Co-Ni (curve 2) all deposited from simple chloride or sulfate baths are used as examples. The outstanding feature of this figure is that the composition curves for the more noble metals, Ni and Fe, lie below the composition reference line, AB, in contrast to curves 1 and 2 of Fig. 2.1, an example for normal co-deposition.

This means that although Fe and Ni are the more noble metals, they are not preferentially deposited. The data for curve 3, representing deposition of Ni-Zn alloys, comes from the work of Schoch and Hirsch [13] which was done in 1907 and is one of the earliest studies of the

principles of alloy deposition. Although the total metal content of their baths varied widely, this does not vitiate the relation between the metal ratio of the bath and the deposit. The behaviour of metals in anomalous co-deposition is not as consistent and clear-cut as would appear from the curves for metals in normal codeposition. Under some conditions of current density and temperature, the metals may co-deposit in a normal fashion and under other conditions in an anomalous fashion.

2.2.4 Effect of Total Metal Content of the Bath on the Composition of the Deposit

Variation of the total metal content of a bath, at a fixed metal ratio, appreciably affects the composition of alloys in regular codeposition but has either slight effect or no uniform trend in irregular, anomalous and induced codeposition.

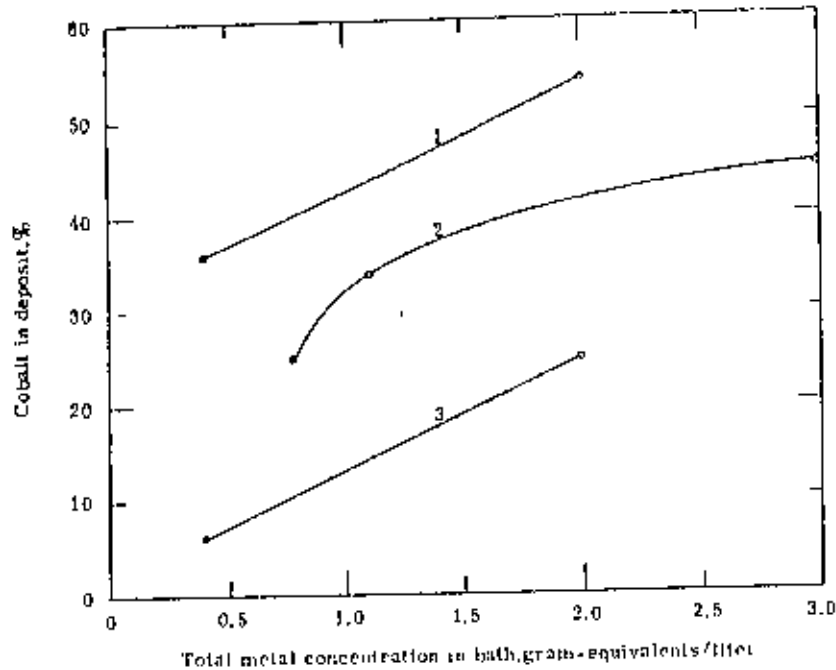


Fig.2.3: Relation between the composition of the deposit and the total metal content of the bath in anomalous co-deposition.

Curves 1 and 3: From the data of Glasstone and Speakman [14].

Curve 2 : From the data of Fink and Lah [15].

The effect of total metal content of the bath on the composition of the deposit in anomalous codeposition is illustrated in Fig. 2.3 with data on the deposition of Co-Ni alloys taken from the work of Glasstone and Speakman [14] and Fink and Lah [15]. The alloys were deposited from simple sulfate baths. Cobalt deposited preferentially although it is less noble than Ni. The curves show that for a sevenfold increase in total metal content of the bath, the cobalt content of the deposit increased only slightly. Comparison of these curves with the much steeper curve 2 of Fig. 2-2 shows the much greater effect of varying the metal ratio of the bath.

2.2.5 Effect of pH of the Plating Bath on the Composition of the Deposit

The effect of pH on the composition of an electrodeposited alloy are specific and usually unpredictable. In some baths, pH has a large effect and in others a small effect on the composition of the deposit. The determining factor is the chemical nature of the metallic compounds, because the pH does not exert its effect directly but by altering the state of chemical combination of the metals in solution. Simple metallic ions are only slightly sensitive to variations in the pH of the solution. On the other hand, the composition and stability of many complexes — in both alkaline and acid solution — are a function of the pH. For example, complexes, such as stannate, zincate, cyanides and amines, which are stable in alkaline solution, decompose when acidified. As a general rule, variations of pH should have little effect on the composition of alloys deposited from baths containing the metals as simple ions and should have a large effect on the composition of alloy deposited from baths in which the parent metals were present as complexes with large instability constants.

Glasstone and Speakman [14] determined the most noble potentials at which the iron-group metals and their mutual alloys deposited from solutions of various pH. They did this by gradually increasing the current density and noting the potential at which codeposition was initiated. As might be expected, the more acid the solution, the higher was the current density

required to initiate metal deposition. However, rather unexpected was the finding that the potential at which deposition was initiated was about the same in the solutions of various acidity, since the potential of initial deposition was independent of the pH of the bath, one might surmise that the composition of the electrodeposited alloys might also be little influenced by variations in pH.

Fig. 2.4 shows data from three sources. Curve 1 represents data from Young and Struyk [12] for the deposition of Co-Ni alloys from a simple salt bath. Curve 2 represents data from Glasstone and Symes [16] for the deposition of Fe-Ni alloys from a sulfate bath. Curve 3 is the data of Raub [17] for deposition of Fe-Ni alloys from a bath containing citric acid. The three curves all represent anomalous codeposition since Ni, the more noble metal, occurs in the deposit in a smaller percentage than its metal-percentage in the bath, which was 90% or more.

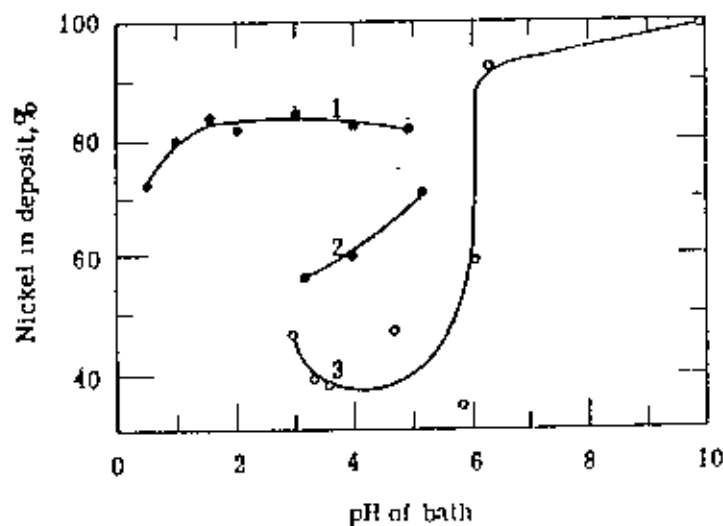


Fig.2.4: Effect of pH on the composition of deposits in anomalous co-deposition.

Curve 1: Cobalt-nickel alloys from the data of Young and Struyk [12]

Curve 2: Iron-nickel alloys from the data of Glasstone and Symes deposited from sulfate bath [16]

Curve 3: Iron-nickel alloys from the data of Raub deposited from a bath containing citric acid [17]

The curves show that the composition of the deposit is little affected by pH up to 5. This is in accord with the surmise based on the work of Glasstone and Speakman, mentioned previously, and in accord with the general proposition that pH has little effect on deposition from baths containing simple metallic ions. The large increase in the Ni-content of the deposit shown by curve 3 is doubtlessly caused by the complexing of the iron with citrate ion, when the pH of the bath was increased above 6.

2.2.6 Relation Between Current Density and Composition of Electrodeposited Alloys

Current density is the most important of the operating variables. The mechanism may be examined from two view points—diffusion control and the cathode potential. According to simple diffusion theory, the rate of deposition of a metal has an upper limit which is determined by the rate at which its ions can move through the cathode diffusion layer. At a given current density, the rate of deposition of the more noble metal is relatively much closer to its limiting value than that of the less noble metal. An increase of current density, therefore, must be borne mainly by an increase in the rate of deposition of the less noble metal. With regard to the cathode potential, an increase of current density causes the cathode potential to become more negative (less noble) and hence this condition should increase the proportion of the less noble metal in the deposit. The situation is however different in anomalous codeposition.

In Fig. 2.5, curve 1 represents the deposition of Fe-Zn alloys from an acid sulfate bath at 90°C. The data are from the work of von Escher and others [18]. The point P indicates the metal percentage Zn in the bath, which is 11.5%. The curve consists of three branches

In the low current density region, from a to b, the codeposition appears to be of normal type, that is, the deposit contains a smaller content of the less noble metal, Zn, than corresponds to

the metal-percentage Zn, P, in the bath, and with increasing current density the content of Zn in the deposit increases. The deposit rapidly increases in Zn content and above 2.5 Amp/dm^2 contains much more Zn than corresponds to the metal-percentage Zn in the bath.

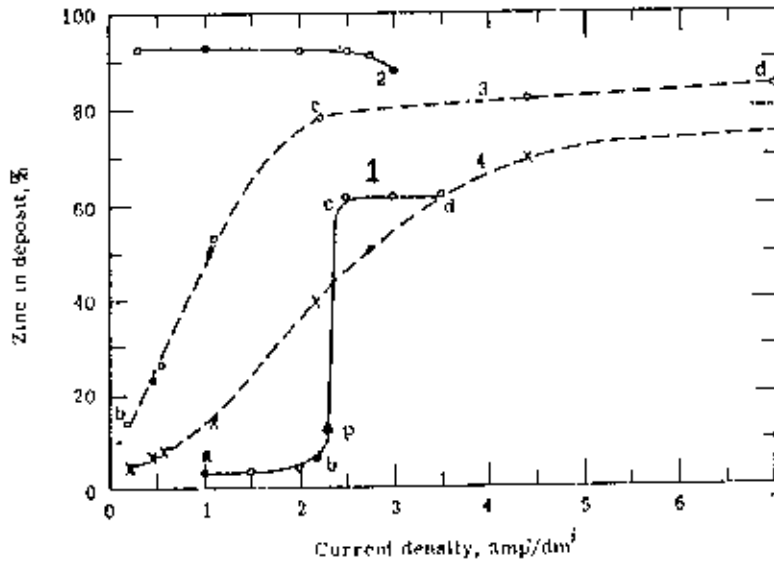


Fig.2.5: Relation between alloy composition and current density in anomalous co-deposition.

Curve 1: Iron-zinc alloys deposited from acid sulfate bath [18]

Curve 2: Nickel-zinc alloys from the data of Schoch and Hirsch [13]

Curves 3 and 4: Nickel-zinc alloys deposited from acid chloride bath [19]

The transition of the Zn content of the deposit from a value well below, to a value well above, the metal-percentage Zn of the bath occurs over a rather small range of current density (branch bc). The current density at the point P is referred to as 'transition current density'.

The third branch of curve 1, from c to d, exhibits little change in alloy composition with current density. Since Zn is depositing preferentially, the cathode film must be relatively more depleted in Zn than in Fe; consequently, the deposition should be under diffusion control and the Zn content of the deposit should tend downwards at still higher current density. This fourth type

of relation, illustrated by branch de, is not shown by curve 1 but is shown by curve 2. Curves 3 and 4 for the deposition of Ni-Zn alloys from an acid chloride bath [19] show only two branches. The low current density region from a to b is missing.

2.2.7 Effect of Bath Temperature on Composition of Electrodeposited Alloys

2.2.7.1 General

The effect of temperature on the composition of electrodeposited alloys may be the net result of changes in several characteristics of the plating system, such as the following:

- (a) **Equilibrium potential:** The equilibrium potentials of the metals may change. This is probably not an important factor since the equilibrium potentials of metals do not change greatly with temperature and furthermore electrodeposition is far removed from equilibrium conditions.
- (b) **Polarization.** The deposition potentials of metals usually become more noble with increase in temperature, because polarization is decreased. Whether the deposition of the more noble or less noble metal is favoured depends on which deposition undergoes the largest decrease in polarization. These effects are specific and, therefore, the effect of temperature, via polarization, cannot be predicted without actual measurements on the deposition potentials of each of the metals.
- (c) **Concentration:** An increase in temperature increases the concentration of metal in the cathode diffusion layer, because the rates of diffusion and of convection increase with temperature. This is the most important mechanism by which temperature affects the composition of electrodeposited alloys. According to the principle of alloy deposition, an increase in metal concentration at the solution cathode interface favours increased deposition of that metal which already was depositing preferentially.

(d) Cathode current efficiency: Temperature may affect the composition of an electrodeposited alloy indirectly through its effect on the cathode current efficiency of deposition of the metals, particularly those deposited from complex ions. For example, an increase in temperature increases the cathode current efficiency of deposition of tin from a stannate bath, and of copper from a cyanide bath. In codepositing Sn or Cu with other metals whose efficiencies of deposition are unaffected by temperature the Sn or Cu content of the deposit will increase with temperature regardless of whether Sn or Cu happen to be the more noble or the less noble metal of the pair.

Of these four factors, (c) and (d) are the most important.

2.2.7.2 Effect of Bath Temperature on Composition of Alloys in Anomalous Codeposition

A complex relation occurs in the variation of alloy composition of anomalous type with the temperature of the bath. The effect of temperature can be qualitatively explained on the basis of two factors namely (i) Polarization and (ii) diffusion phenomenon. These two factors have opposite effects on the deposit composition. With increasing bath temperature, factor (i) favours a decrease and factor (ii) an increase in the content of the less noble metal in the deposit. These two opposing influences are responsible for the apparently inconsistent and rather indeterminate trends of alloy composition with temperature in anomalous codeposition.

The influence of polarization is especially important in anomalous codeposition, since the failure of the more noble metal to deposit preferentially may be construed as indicative of some kind of large polarization in the deposition of this metal. If this be granted, then the reduction of polarization which occurs on raising the temperature of the plating bath should be larger for the more noble metal and the deposition of the latter should be favored to a larger extent than

that of the less noble metal. Hence, in anomalous codeposition, the content of the more noble metal in the deposit may increase with temperature.

An increase in temperature favours the deposition of that metal which is preferentially deposited, because it speeds up diffusion and thus relieves the depletion of metal at the cathode. Since in anomalous codeposition, the less noble metal deposits preferentially, an elevation of temperature should increase the content of the less noble metal in the deposit.

2.2.8 Effect of Agitation of Bath or Rotation of Cathode on the Composition of Electrodeposited Alloys

Agitation of an alloy plating bath or rotation of the cathode can directly affect the composition of the alloy by reducing the thickness of the cathode diffusion layer. This is a purely mechanical action which does not change the electrochemical properties of the solution or the mechanism of the plating process. Being of this nature, agitation has a more consistent influence on the composition of the deposit than either temperature or current density.

The effect of agitation on the composition of the deposit is due to the concentration changes which it produces at the cathode-solution interface. During alloy deposition, the cathode diffusion layer is depleted in metal ions and furthermore, the ratio of the concentrations of the metals in the layer differs from that in the body of the bath. Agitation of the bath or rotation of the cathode, by decreasing the thickness of the cathode diffusion layer not only results in an increase in the concentration of metal ion in the cathode diffusion layer, but also causes the metal ratio of the diffusion layer to approach more closely to that of the solution in the body of the bath. This favours an increased rate of deposition of that metal which is already depositing preferentially. The effect of agitation, thus, is similar to that of increasing the concentration or the temperature of a bath.

2.3 PROPERTIES OF ELECTRODEPOSITED ALLOYS

The utilization of metals is determined by their properties and by economic considerations. With the growth of technology, however, electrodeposits began to be applied to a variety of engineering and scientific purposes and, consequently, more interest was shown in their properties. Obviously, the extension of the applications of electrodeposits would be greatly accelerated if more information were available concerning their mechanical, physical and other properties.

The properties of electrodeposited metals may be varied by altering the conditions of deposition. Indeed, some of the properties of electrodeposited metals, for example, the hardness, may be made to vary over a much wider range than those of thermally prepared alloys. Again, the properties of electrodeposited metals may be varied further by application of heat treatments.

2.3.1 Mechanical Properties of Electrodeposited Alloys

2.3.1.1 Hardness

The hardness of electrodeposits is usually measured by indentation or scratch methods. The use of a pointed diamond indenter, such as a Vicker or Knoop diamond, in conjunction with a light load of 25 to 250 gm is the preferred method. The measurements are usually referred to as the microhardness but they differ from ordinary indentation methods only in that a lighter load is used. The indentations are usually made on a polished cross section of the deposit, which should be a minimum of about 50 μm thick, but measurements can also be made directly on the plated surface parallel to the basis metal.

The hardness of electrodeposited metals is greater than that of cast metals, and in turn the hardness of electrodeposited alloys is greater than that of either of the individually deposited

parent metals. This is illustrated in Table 2.2 for several alloys. It is of interest to note that although tin is much softer than copper the hardness of the electrodeposited alloys are greater than that of copper and the hardness increases with the content of tin to a value 450 Brinell at 45% tin.

Table: 2.2

Comparison of Hardness of Electrodeposited Alloys with that of Individually Electrodeposited Metals and with that of Metallurgical Metals.

No.	Alloys/ Metals	Nature of Metal	Composition, %	Hardness	
				No.	Method
1.	Tin	Metallurgical	100	4	Brinell
2.	Tin	Electrodeposited	100	8	Brinell
3.	Copper	Metallurgical	100	60	Brinell
4.	Copper	Electrodeposited	100	45-80	VPN
5.	Bronze	"	12, Sn	222	Brinell
6.	"	"	17, Sn	345	"
7.	Speculum	"	45, Sn	450	"

The hardness of electrodeposited alloys increases most rapidly with the first small additions of the alloying metal, then at a decreasing rate. The percentage of alloying element above which the hardness shows little change, depends on the nature of the alloy. For example, the hardness of electrodeposited cobalt-tungsten alloys increased with tungsten content until the latter reached 35-50%. In contrast, the hardness of electrodeposited silver-lead alloys reached its

unit when the lead content of the alloy was about 3%, as shown in Fig. 2.6. These data are from Raub [20].

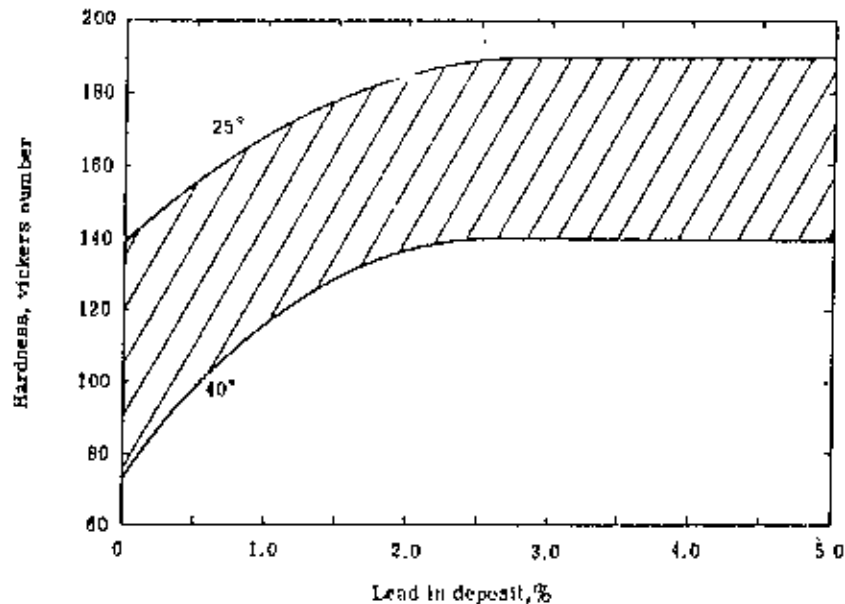


Fig.2.6: Effect of Pb content on hardness of Ag-Pb alloys deposited from a cyanide-tartrate type of bath. One set of specimens was deposited at 25°C, the other at 40°C. The curves are actually boundaries of the data with points falling in between, since the hardness measurements showed considerable scatter.

2.3.1.2 Ductility

Ductility is the amount of abuse that a coating can withstand before cracking or before becoming separated from the basis metal. Many tests have been developed to measure ductility. They are tensile test, bulge test, stretching test, low frequency fatigue test, bend test etc. Of them, the most widely used approach is some type of bend test in which coated material is deformed in a standardized manner while the coating is scrutinized for the first evidence of cracking or peeling.

Ductility depends on coating composition, coating thickness, surface roughness of the coating, overpotential and other coating characteristics. The ductility decreases with increasing surface

roughness, provided other parameters which influence the ductility are kept constant [21]. Except for very ductile deposits, the apparent ductility is an inverse function of the coating thickness [22]. For systematic study of ductility dependence on coating composition, the other parameters must be identical.

2.3.1.3 Wear Behaviour

Wear may be defined as unintentional deterioration resulting from use or environment. It may be considered essentially a surface phenomenon. Wear is one of the most destructive influences to which metals are exposed. The displacement and detachment of metallic particles from a metallic surface may be caused by contact with (i) another metal (adhesive wear), (ii) a metallic or a non-metallic (abrasive wear), or (iii) moving liquids or gases (erosion).

It is generally accepted that a universal wear test is not feasible. Equipment for wear testing must be designed to simulate actual service conditions. These tests should have proved reproducibility and should be validated by correlation with service data. The pin-on-disc tester is a means of evaluating wear resistance because a flat loaded pin is in rubbing contact with a flat rotating disc. During the tests, the sample (pin) is pressed against the rotating disc under a constant load for a prespecified time period. Pins are weighed before and after the tests to determine the weight loss due to wear. The extent of weight loss is inversely proportional to wear resistance.

Hot dip zinc coating is applied to steel components for its anti-corrosion property. Zn-Ni alloy coating has been found to possess even more improved corrosion resistance. Nickel being a rather expensive element, a fairly thin (~30 μm) Zn-Ni alloy coating is usually applied on steel. The dirt particles of the environment or other abrasive agents can cause wear of coated components. As hot dip zinc coating is quite thick (several hundred μm), wear to some extent does not expose the steel substrate to environment. On the contrary, wear can remove thinner

Zn-Ni alloy coating resulting in faster corrosion of the substrate unless it possess adequate wear resistance. In the present study wear behaviour of different Zn-Ni alloy coatings has been studied and compared with those of pure zinc coatings.

2.3.2 Protective Value of Alloy Coatings

2.3.2.1 General Considerations

The most important use of electrodeposits, whether individual metals or alloys, is as coatings to protect other metals, such as steel, brass and zinc from corrosion. For this reason the main interest in the chemical properties of electrodeposited alloys has centered around the corrosion and tarnish resistance of the alloys with particular emphasis on the protection that alloy coatings afford to steel.

The chemical reactivity of a binary alloy usually lies between that of its constituents and at first sight it would seem as if electrodeposition of the alloy would be of no advantage, since its corrosion resistance would be inferior to that of its more noble constituent. This would be true if the alloys were used in the massive state, but when applied as coatings their chemical reactivity is only one of the factors that determines their applicability as a protective coating, other important considerations are the nature of the basis metal, thickness and continuity of the coating and the service conditions.

To show that the chemical nature of a metal alone does not determine its value as a coating, it may be pointed out that, for the protection of steel against corrosion, metals of diametrically opposite degrees of chemical reactivities are utilized; yet each type satisfactorily affords protection against corrosion but in different applications. The two types of coatings which are applied to steel are designated as cathodic and anodic. Cathodic coatings, of which nickel and copper are examples, are chemically less active than steel. In a salt solution these metals are

positive (less active) to steel. Coatings of these metals protect steel by shielding it from corrosive environments and are effective as long as they completely envelope the steel.

Being less reactive than steel, a given thickness of coating lasts much longer than an equivalent thickness of steel. However, if discontinuities extending down to the steel occur in the coating, the corrosion of the steel is accelerated by the galvanic action which is set up between the coating as cathode and the steel as anode in the presence of moisture.

In contrast to the cathodic coatings, the anodic coatings, of which zinc and cadmium are the most important, are more active than steel. In a salt solution these metals are negative (less noble) to steel. Anodic coatings protect steel from corrosion initially, just as do the cathodic coatings, by shielding it from corrosive environments, but being chemically active they are attacked more rapidly than cathodic coatings. When, or if, the steel is exposed through discontinuities in the coating, the latter still protects the steel by virtue of a galvanic action. In the presence of moisture the coating becomes the anode of a galvanic cell and is slowly consumed, whereas the steel being cathodic does not corrode, until the exposed area becomes so large that parts of it are too far removed from the coated area to receive appreciable current.

Zn-Ni alloy coatings provide better corrosion protection of steel than other zinc coatings. In recent years, the commercial use of these alloys has greatly expanded, replacing Zn and Cd plating in many applications such as in automotive body panels. Maximum corrosion protection from rust is afforded by Zn-Ni alloy coatings in the range (11-14)% Ni [23].

2.3.2.2 Advantages of Using Alloy Coatings and Examples of Corrosion Resistant Alloy Coatings

Since the chemical reactivity of alloys usually falls between that of the parent metals, it is necessary to consider if there are any advantages in using a coating of an alloy rather than a coating of either one of the parent metals. There are three possible advantages of using alloys.

(1) Since corrosion conditions are rather specific, often a certain composition of alloy yields better protection in a particular environment than a pure electrodeposit. Or stated in another way, the composition of the alloy may be tailored to meet a particular kind of corrosive condition.

(2) Metals with good corrosion characteristics which cannot be deposited alone can be obtained as alloys in induced codeposition.

(3) If one of the parent metals is expensive, the use of an alloy affords an economy.

Point (1) is the most important consideration that determines whether an alloy is used instead of an individual metal. The Zn-Sn alloys are cited as an example of tailoring a deposit to meet a corrosive condition. Zinc protects steel sacrificially, but being rather active does not have a long life. On the other hand, tin is less active than steel and on outdoor exposure protects it mechanically for cathodic coatings. The protective value of an electrodeposited coating of an alloy containing 80% of tin and 20% of zinc is superior to that of either of the parent metals. Apparently, the presence of the less active tin decreases the rate of anodic attack of zinc by just the right amount, so that the coating still protects steel anodically and yet has a longer life than pure zinc coatings. Another examples of the beneficial effect of alloying is the protective value of chromium-iron alloy. Chromium alone is so passive that it functions on steel only as a cathodic type of coating, and rusting readily takes place through cracks in the coating. However, the coating obtained by codepositing chromium with about (5-10)% iron is sufficiently active to protect steel galvanically in the salt spray.

As an explanation of point (2), elements like W, Mo and P resist attack by acids and other chemical reagents and confer some of their corrosion resistance on their alloys. A few examples of the effectiveness of coatings of these alloys against corrosion are cited. Coatings

of Co-W alloy provides outstanding protective value to steel in outdoor exposure tests. Although the coatings became dark and discoloured, they prevented formation of rust and were superior to either pure nickel or pure cobalt coatings. Ni-P alloys [24] in outdoor exposure tests remained bright much longer than nickel deposits, and a coating of the alloy about 12 μ m thick was in as good condition at the end of the test as a coating of nickel of twice the thickness.

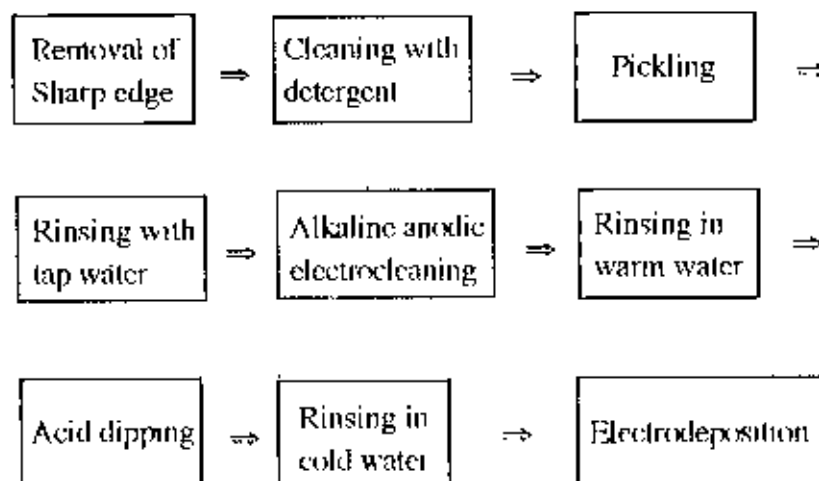
CHAPTER: THREE

3. EXPERIMENTAL**3.1 Materials**

Commercial mild steel sheets were used as substrates in this investigation. As anodes for electrodeposition, lead sheets were used. The size of lead anodes was 50 mm x 25 mm x 1 mm and that of mild steel substrate was 60 mm x 30 mm x 1 mm.

3.2 Preparation of Specimen for Electrodeposition

The flow diagram of sample preparation is as follows:



Removal of sharp edges: This is done by grinding the sharp edges. Current density becomes larger at sharp edges and this, in turn, results thicker deposition at the edges. In order to get uniform deposition, sharp edges were removed.

Cleaning with detergent: The sample may contain grease, oil, drawing compounds and other substances which come during its fabrication. If these contaminants are present, they will weaken the next pickling action on the sample. So, these were removed. For this operation, commercial Na_2CO_3 powder were used.

Pickling: Pickling was done for the chemical removal of surface oxides (scale) and other contaminants such as dirt from metal by immersion in an aqueous acid solution. Particulars of pickling operation are given in Table 3.1.

Rinsing: Thorough rinsing was done for obtaining the clean, stain-free and smut-free surface necessary for subsequent electrocleaning operation. In order to get optimum rinsing conditions, maintenance of the high pressure cold water sprays were provided. Thus, acid contamination of the subsequent electrocleaning bath is eliminated or minimized.

Anodic Electrocleaning: Here the sample was used as anode in an alkaline bath. Mild steel plate of size 60 mm x 30 mm x 1 mm was used as cathode in this operation. This treatment removes metallic oxides and smuts and prevents the deposition of other positively charged metallic ions, which otherwise may result in a detrimental film on the work piece. The particulars of this operation are given in Table 3.1.

Rinsing in warm water: Alkaline cleaners are difficult to rinse. Carryover of residues can produce staining, skip plating or loss of adhesion. So warm water was used in rinsing of the electrocleaned sample.

Acid dipping: Plating is initiated on an active surface. So, electrocleaned samples were acid dipped to neutralize any residual alkali film, remove oxides and smuts and to activate the workpiece for subsequent electroplating. Various parameters of this treatment are given in Table 3.1. The sample is now ready for electrodeposition.

Table 3.1

Particulars of Pickling, Electrocleaning and Acid Dipping Operations

Name of operation	Reagents used (Wt.%)	Operating conditions		
		Temp. (°C)	Current density (mA/cm ²)	Time
Pickling	H ₂ SO ₄ : 20 H ₂ O : 80	70		10 Mins.
Anodic electro-cleaning	NaOH : 50 Na ₂ CO ₃ : 25 Na ₂ SiO ₃ : 20 Na ₅ P ₃ O ₁₀ : 05	60	55	02 Mins.
Acid dipping	HCl : 10 H ₂ O : 90	Room		15 Secs.

3.3 Electrodeposition Set-up

Electrodeposition was carried out in a laboratory type electrodeposition set-up consisting of a beaker, a D.C. power supply, a thermometer, a magnetic stirrer, a stand and perspex holder. The beaker containing the electroplating solution and magnetic stirrer was placed on a magnetic hot plate so as to be able to agitate the electrolyte automatically. Anode and cathode were connected to the D.C. power supply via a milliammeter. Two anodes were used on both sides of the cathode for uniform deposition on both sides of the cathode. Schematic of the set-up used for electrodeposition is shown in Fig. 3.1.

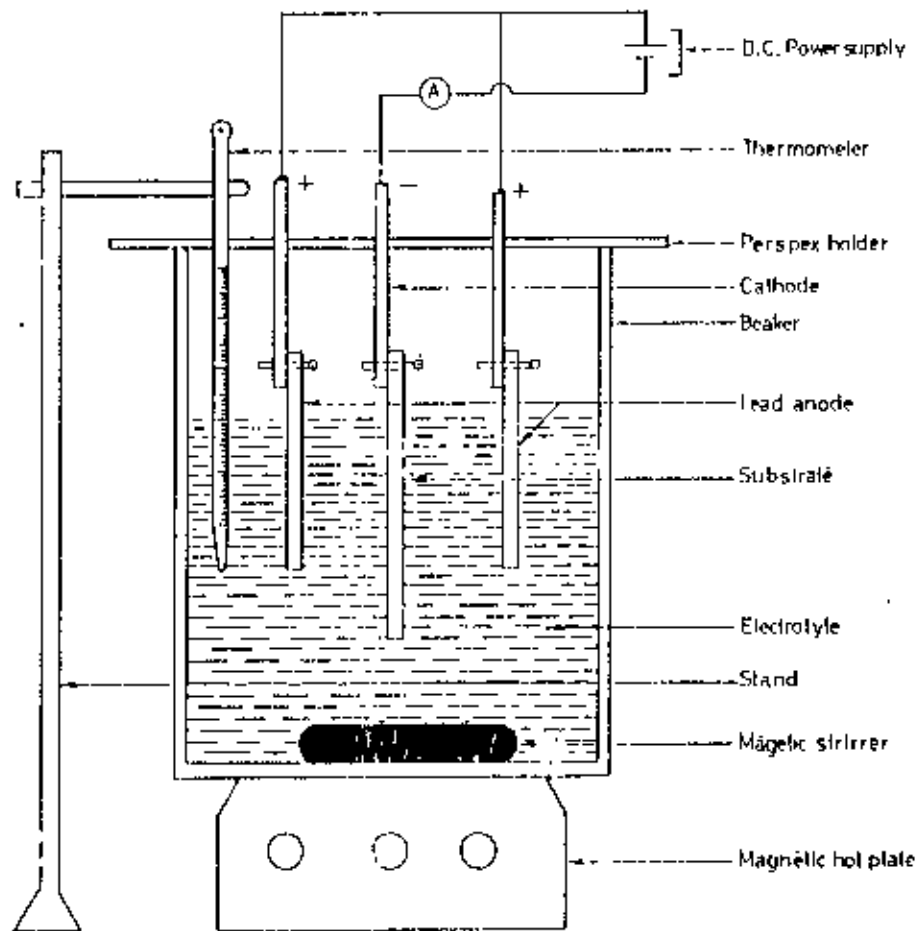


Fig. 3.1: Electrodeposition unit

3.4 Electroplating Operation

The beaker was filled to approximately two thirds of its marking point with bath solution. All the accessories were then set-up. The prepared substrate was then connected to the negative terminal of a D.C. power supply and two lead anodes to the positive terminal. A digital multimeter was also placed in the circuit to measure the current. Deposition was carried out at constant current densities viz. 50, 75, 100, 150, 200 mA/cm². At the end of electrodeposition for a predetermined time period e.g. 30, 60, 90. minutes etc., the power supply was switched off and the workpiece was taken out. After deposition, the specimens were thoroughly rinsed in cold water to remove surplus electrolyte. After rinsing, the specimens were dried and stored

in a desiccator for further investigation. Compositions of different baths used are given in Table 3.2.

Table 3.2

Plating bath compositions for the electrodeposition of Zn metal coating and various Zn-Ni alloy coatings.

Bath components	Bath concentrations (g/L)			
	Pure Zn	Zn-Ni alloy		
	Bath 1	Bath 2 [30]	Bath 3 [30]	Bath 4 [30]
NiSO ₄ ·6H ₂ O	-	285	350	200
ZnSO ₄ ·7H ₂ O	240	150	150	10
H ₃ BO ₃	-	-	-	35
NH ₄ Cl	15	-	-	-
Na ₂ SO ₄	-	150	150	-

3.5 Electrodeposition to Constant Thickness

Both wear resistance and ductility are functions of coating thickness. So depositing film of constant thickness is necessary. Deposition of 40 μm thickness and 20 μm thickness was made from all types of baths for wear test sample and ductility test sample respectively. Theoretical time required to make a film of 40 μm thickness was calculated from Faraday's law. As current efficiency always remains less than 100%, practical thickness will be lower than the theoretical value. To obtain a deposit of 40 μm thickness, several deposits were made by varying the deposition time e.g. 1.2t, 1.4t, 1.6t etc. (t=theoretical time for 40 μm thick film) for a fixed bath. The thickness of the deposits were measured under an optical microscope. A graph was

drawn by taking time as abscissa and thickness as ordinate. From the graph, the point representing $40 \mu\text{m}$ thickness was located and the corresponding time was obtained. Then deposits of $40 \mu\text{m}$ thickness were made for the time already obtained. Fig. 3.2 shows the actual time required to obtain $40 \mu\text{m}$ thick deposit. Deposition to $20 \mu\text{m}$ thickness was also performed in the similar way.

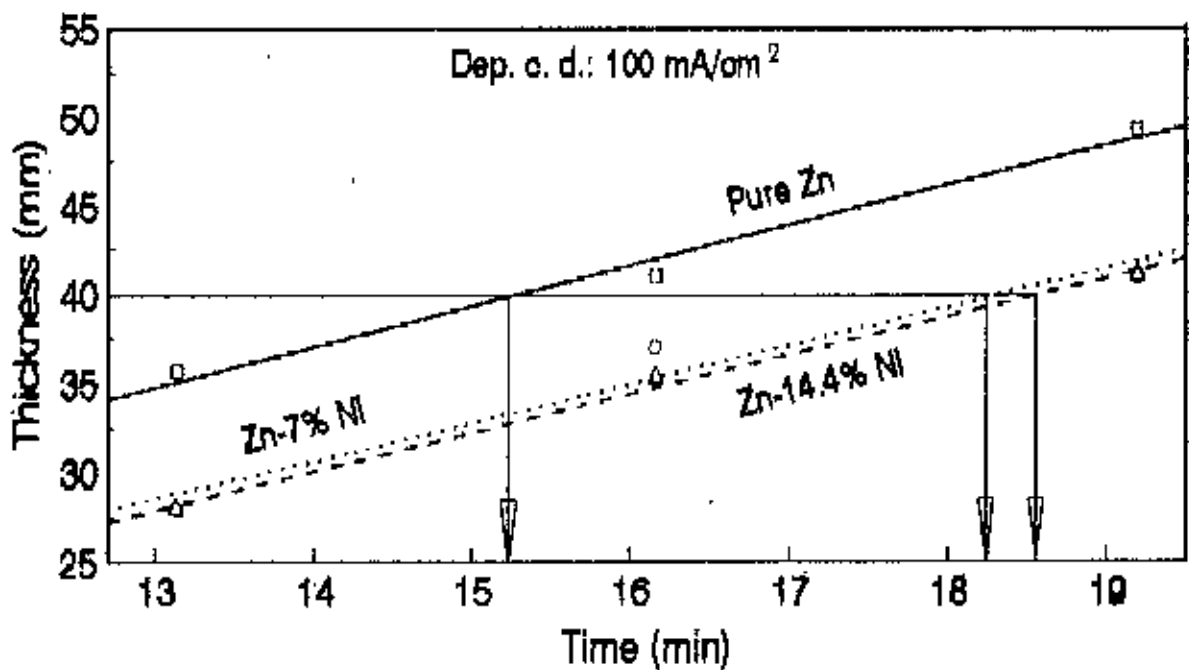


Fig.3.2: Time calculation for $40 \mu\text{m}$ thick deposit

3.6 Methods of Investigation

In the present study, the following tests have been conducted on the deposit:

- i) Chemical analysis of the coating
- ii) X-ray diffractometry of both as deposited and annealed coating
- iii) Microhardness measurement of both as deposited and annealed coating
- iv) Wear test of the deposit
- v) Ductility test of the coating.

3.6.1 Chemical Analysis of the Zn-Ni Alloy Deposit

Chemical analysis of the deposit was carried out by the conventional wet method [31]. Weight of the electrodeposited sample was taken first (say w_1). The deposit was allowed to dissolve in 150 c. c. conc. HCl solution. Precaution was taken here so that HCl do not react with the substrate. The sample was rinsed with tap water, dried in acetone and weighted (say w_2). So, $w_1 - w_2 (=w, \text{ say})$ gives the weight of the deposit dissolved in HCl solution. The solution was then heated until the volume reduced to 100 c.c.

At neutral point, dimethyl glyoxime ($C_4H_8N_2O_2$) was added. Ni-glyoxime precipitate of blood red colour was formed which was separated by filtering through a dual filter paper of equal weight. The filtrate was treated several times with NH_4OH , dimethyl glyoxime in sequence until precipitation was completed. The precipitate was then washed several times with hot water, dried for one hour at $110-120^\circ C$ and weighed as $NiC_8H_{14}O_4N_4$. All types of samples were taken under this treatment and Ni% was determined.

3.6.2 Wear Test

Wear tests were carried out in a pin-on-disc type apparatus (Fig. 3.3) under dry sliding conditions in the ambient air at room temperature. Cylindrical pins of 8 mm diameter and 6.5 mm length coated with 40 μm thick deposit were used. Grey cast iron discs of 80 mm diameter and about 10 mm thickness were used as the counter body.

During the tests, the sample was pressed against the rotating disc under a constant load for a prespecified time period. Loads of 120, 175 and 250 gm were used during the tests. Testing period were 5, 10, and 15 minutes. The counter body was rotated at 500 rpm which gave a linear speed of 1.39 m/s. For each experiment, a new pin and a new disc were used. Before the tests, both the pin and the disc were degreased, cleaned thoroughly in water and dried

immediately in acetone. After testing, the worn surface of the pins was examined by optical microscopy and the width of the wear scar was measured. At least three tests were carried out for each set of conditions and the average width of wear scar on the coated pin was taken as a measure of the coating wear.

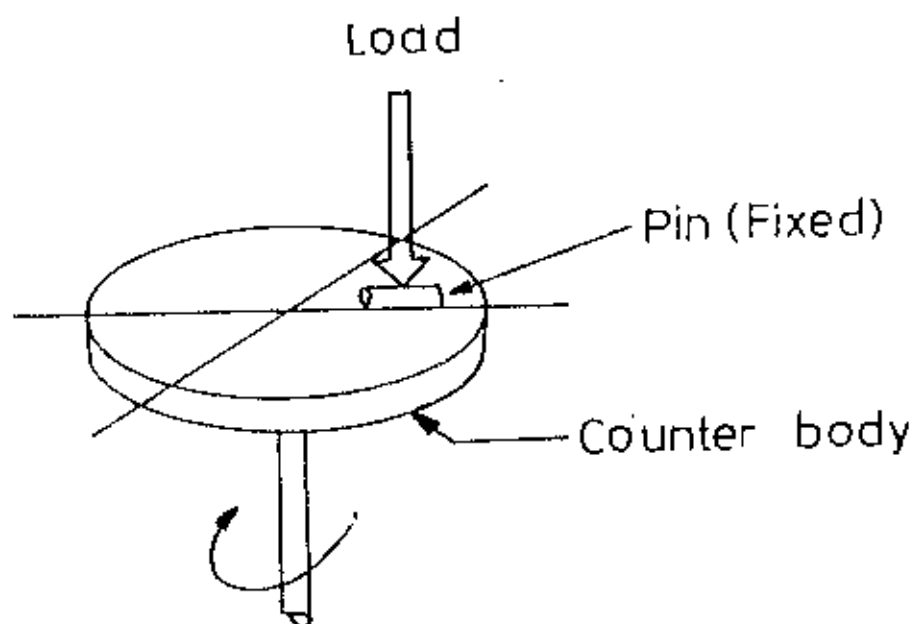


*Fig.3.3: Schematic diagram of wear test apparatus.
(Pin-on-disc type)*

3.6.3 Micro-hardness Measurement

Microhardness values were determined by using a Shimadzu microhardness tester. Microhardness measurements were carried out by using 50 gm load applied for 5 seconds on lightly polished and unetched specimen. Microhardness measurements were done for all deposits of various composition

Microhardness was also taken after annealing the samples at 325°C for 1/2 hour for samples deposited from Bath 2 and Bath 3 and at 700°C for 1/2 hour for sample deposited from bath 4.

Annealing temperatures were selected from the equilibrium phase diagram of Zn-Ni alloy as shown in Appendix A

3.6.4 Phase Study through X-ray Metallography

Phase structures of both as-deposited and heat-treated coatings were investigated by means of X-ray diffraction and compared with the equilibrium phase diagram (Appendix A). The operating condition of X-ray diffractometer is shown in Table 3.3.

Table 3.3
Operating condition of X-ray Diffractometer

Radiation	: CuK α
Voltage and Current	: 30 KV, 15 mA
Scanning speed	: 2 $^{\circ}$ /min
Chart speed	: 10 mm/min
Range	: 30 $^{\circ}$ - 90 $^{\circ}$

3.6.5 Ductility Test

Bend test for ductility of plated metals was performed in accordance with ASTM B 489-68 [22]. A series of mandrels with diameters from 6 to 50 mm in 3 mm steps with length of 150 mm were used for the test. Flat specimens of size 150 mm x 10 mm x 1 mm [22] were cut by a Guillotine shear from the middle portion of electrodeposited sample of size 150 mm x 60 mm x 1 mm. The largest mandrel was placed in the vise. The test specimen, with the better coating outward, was bent over the mandrel so that as the bend progressed the test specimen remained in contact with the top of the mandrel. Bending was continued with slow, steadily applied pressure until the two legs were parallel. If there were no cracks visible under a 10X magnifier, the test was repeated, using new specimens, on progressively smaller-diameter

mandrels, until cracks appeared across or through the plating. The preceding mandrel diameter was taken as the value for the ductility determination. The elongation is determined as follows:

$$E = 100T/(D+T)$$

Where, E = Percentage elongation

T = Total thickness of the basis metal and deposit

D = Diameter of the mandrel

As ductility differs with coating thickness variation, all the specimens taken under this test contained 20 μm thick deposit.

CHAPTER: FOUR

4. RESULTS AND DISCUSSIONS

4.1 Electrodeposition of Zn-Ni alloy Coating

Electrodeposition of Zn-Ni coatings was carried out in three different baths containing different relative proportion of $ZnSO_4$ and $NiSO_4$ (Table 3.2). It was found that pH of the bath had a profound effect on the nature of Zn-Ni alloy deposit. Uniform, adherent coatings were obtained in the pH range of 1.8-3. In baths of $pH > 3$, coating became non-adherent and brittle. At baths of $pH < 1.8$, deposit could form only near the edges while major portion of the substrate surface remained bare.

It is thought that at $pH < 1.8$, Zn-Ni plating baths became too corrosive and therefore attacked the deposited Zn-Ni alloy chemically. At the mid portion of the sample where current density is lower than the average, rate of this chemical attack is higher than the deposition rate. On the other hand, at areas near the edges which receive more current than the average, the rate of deposition is higher than that of chemical attack. As a result, significant amount of deposit could only be seen near the edges at pH lower than 1.8. Referring to the Pourbaix diagram of nickel [33], it is seen that precipitation of $Ni(OH)_2$ can take place at pH greater than 5.8. Due to hydrogen discharge at the cathode, hydrogen concentration at the cathode diffusion layer is lowered and thus pH at the diffusion layer can be increased [34]. Under this condition, pH of

solution of cathode diffusion layer might be greater than 5.8, although pH of the bulk solution remained a slight above 3. As a result $\text{Ni}(\text{OH})_2$ can precipitate in the diffusion layer. Inclusion of this basic hydroxide into the deposit is believed to cause the brittleness of Zn-Ni alloys obtained from bath having pH greater than 3.

Chemical analysis have shown that baths 2, 3 and 4 (Table 3.2) yield Zn-Ni alloys with 7, 14.4 and 40% nickel respectively. The influence of Ni^{2+} concentration in the bath on the composition of the deposit is shown in Fig. 4.1. The position of the curves in this figure shows that under the electrolysis conditions used, zinc is the most readily deposited metal. The percentage of zinc, the less noble metal, in the deposit is always higher than its percentage in solution. While the percentage of nickel, the more noble metal, in the deposit is always lower than its percentage in solution. From this deposition pattern, it is seen that Zn-Ni alloy coating is of anomalous type [25,35].

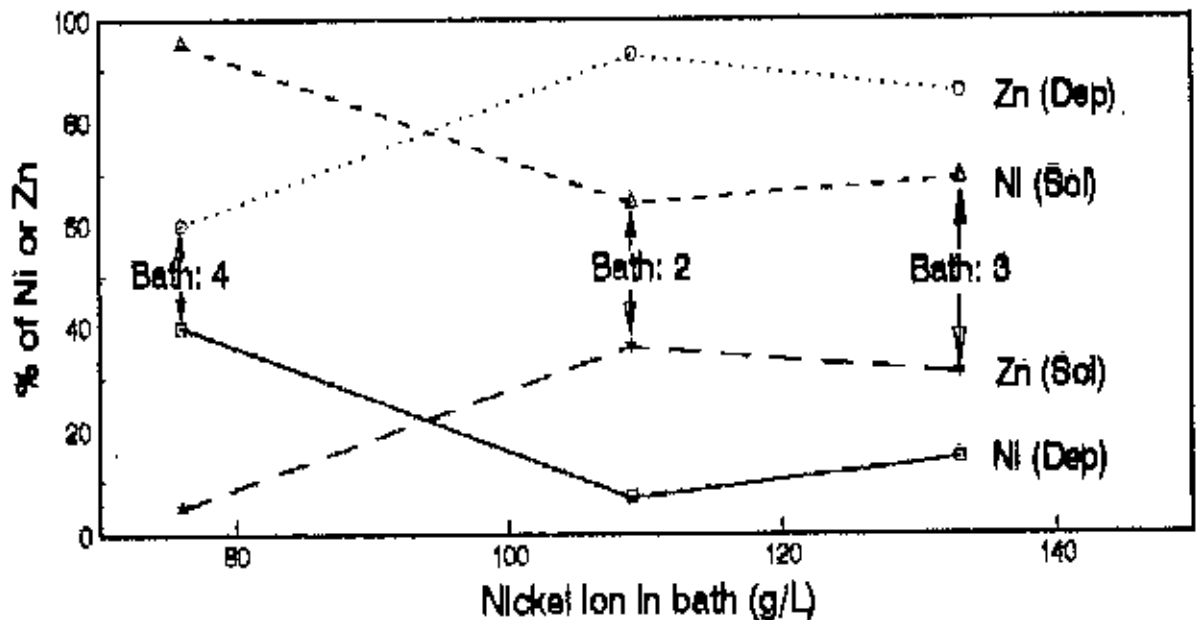


Fig.4.1: Effect of Ni^{+2} concentration in bath on deposit composition

When the percentages of nickel in the deposits and in the baths are related, a linear dependency is obtained. This linear relation is shown in Fig. 4.2. This is well documented with the work done by others [36] who studied electroplating of Zn-Ni alloy films from a chloride bath.

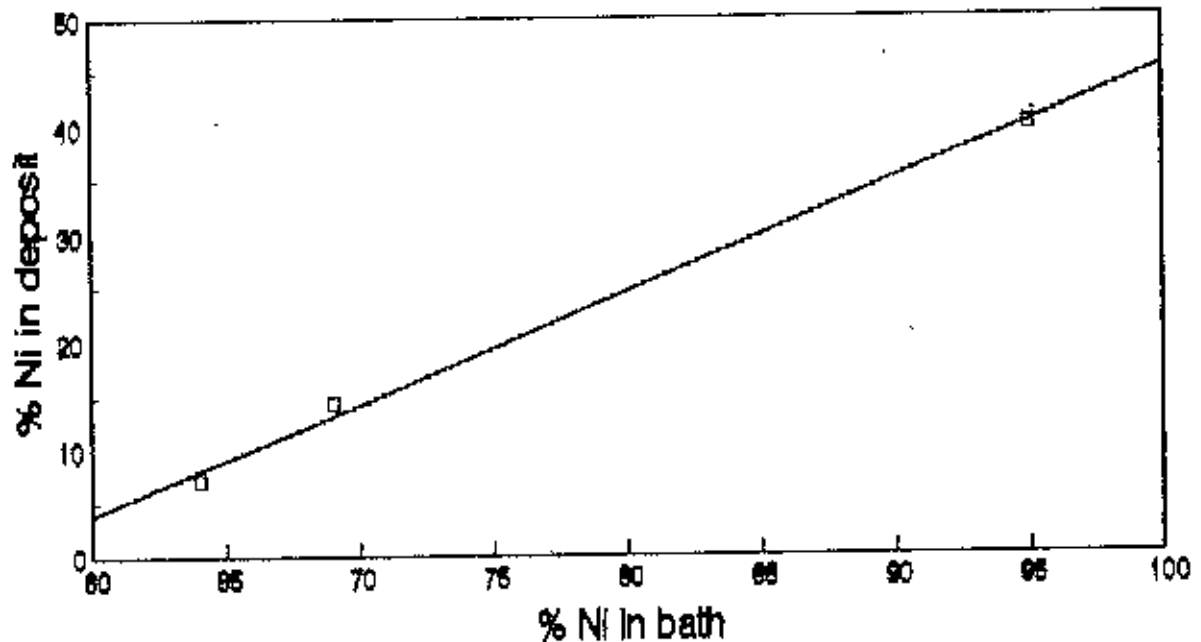


Fig.4.2: Effect of Ni% in bath on Ni% in deposit

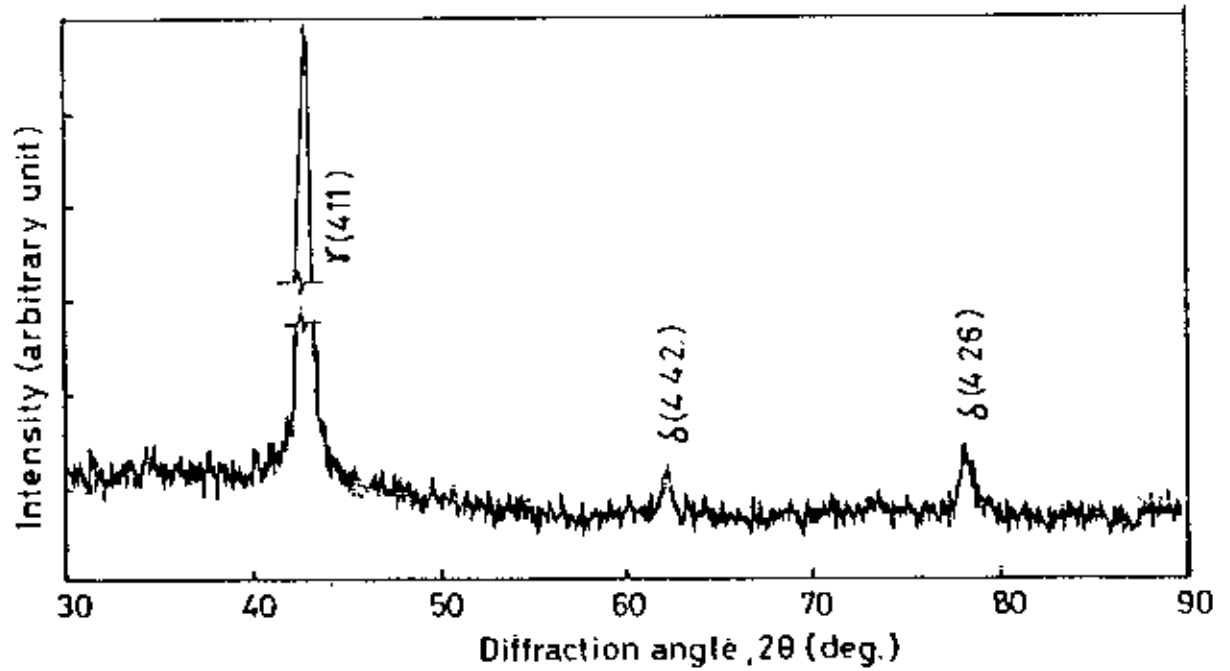
4.2 X-ray Investigation

Each of the three Zn-Ni alloy coatings containing 7% Ni, 14.4% Ni and 40% Ni were analyzed by X-ray diffraction under as-deposited as well as annealed conditions. X-ray diffraction was also performed on as-deposited pure zinc coating. Fig. 4.3 shows the diffraction patterns of Zn-14.4%Ni alloy coating under both as-deposited and annealed conditions. Three prominent diffraction peaks at the 2θ value of 42.6° , 62.3° and 78° are detected for as-deposited sample. These peaks correspond to (111) plane of γ , (442) and (426) planes of δ respectively. The presence of γ and δ -phases is expected for the composition Zn-14.4%Ni from Zn-Ni equilibrium phase diagram as given in Fig. 3.3. The aforesaid three peaks were also detected on the annealed Zn-14.4% Ni alloy coating. Several extra peaks of γ and δ -phase were also

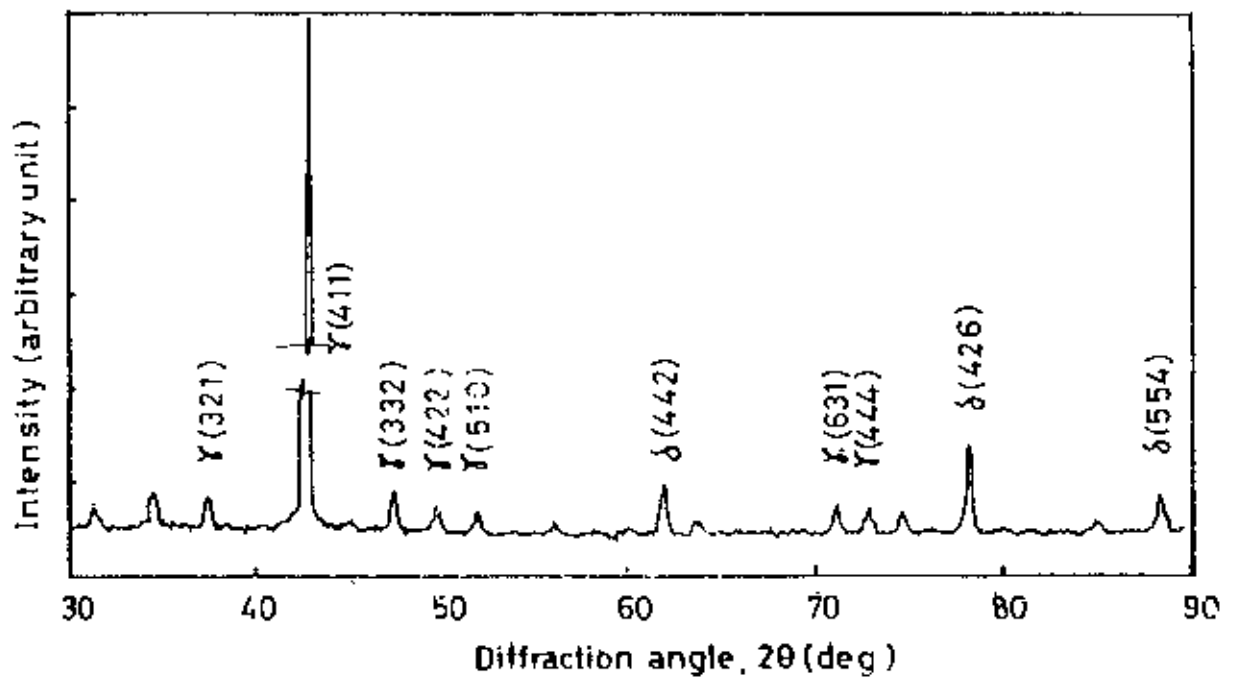
detected. The coincidence of the Zn-Ni equilibrium phase diagram with both the as-deposited and annealed X-ray diffraction pattern indicates that the Zn-14.4% Ni alloy deposited with equilibrium phases in its microstructure. It is to be noted that for annealed sample, three diffraction peaks corresponding to the 2θ value of 31.5° , 34.6° and 74.6° are present which could not be indexed.

As has been stated earlier, only three prominent peaks are observed for the as-deposited sample whereas the diffraction pattern of the annealed sample exhibits the prominent as well as numerous weaker peaks. The absence of weaker peaks in the diffraction pattern of as-deposited sample is believed to be due to finer grain size and presence of internal stress in this sample [37].

Fig. 4.4 shows the X-ray diffraction patterns of Zn-40% Ni alloy coating. Four diffraction peaks, corresponding to the (101) plane of β , (422), (444) and (552) planes of γ phases respectively were detected on both the as-deposited and annealed coating. The peaks representing β and γ -phase agree well with the Zn-40% Ni composition of the Zn-Ni equilibrium phase diagram. The deposition is supposed to be under equilibrium condition due to this well-agreement with the Zn-Ni equilibrium phase diagram. With some extra peaks of γ -phase, three unknown peaks were also detected on the annealed sample. The presence of extra known peaks of annealed sample may be due to its stress-free grains of larger size and favourable orientation [37]. The reason for the presence of the undetected peaks in annealed sample could not be known.

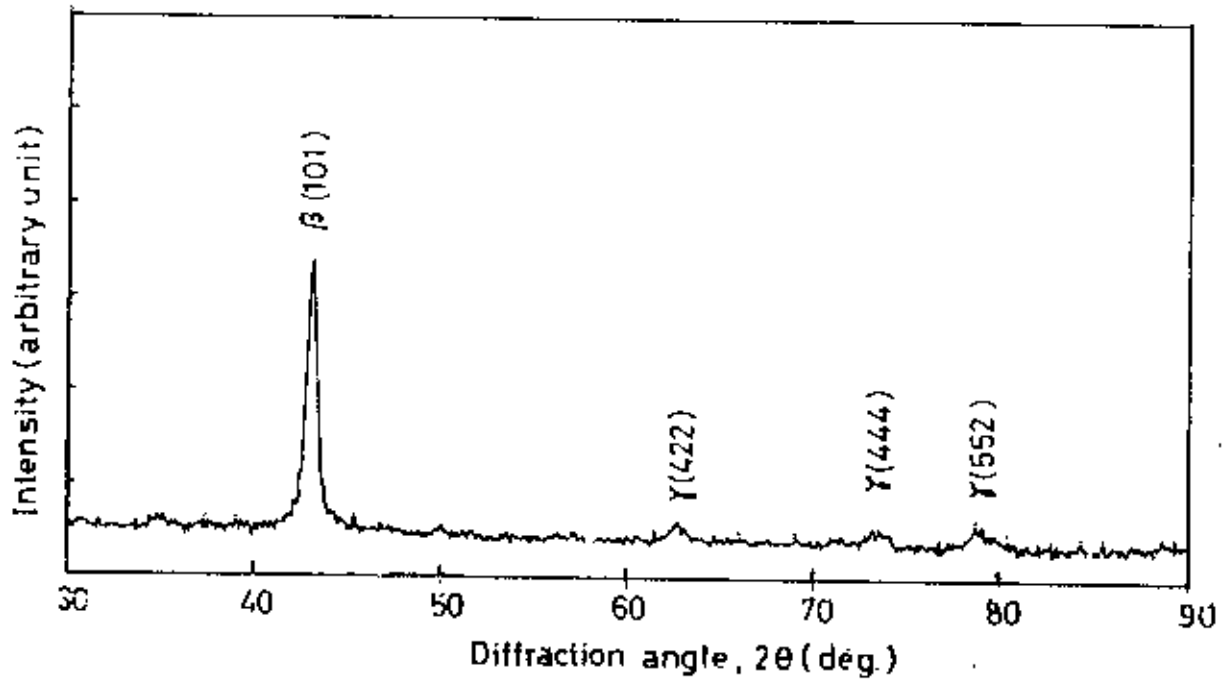


(a)

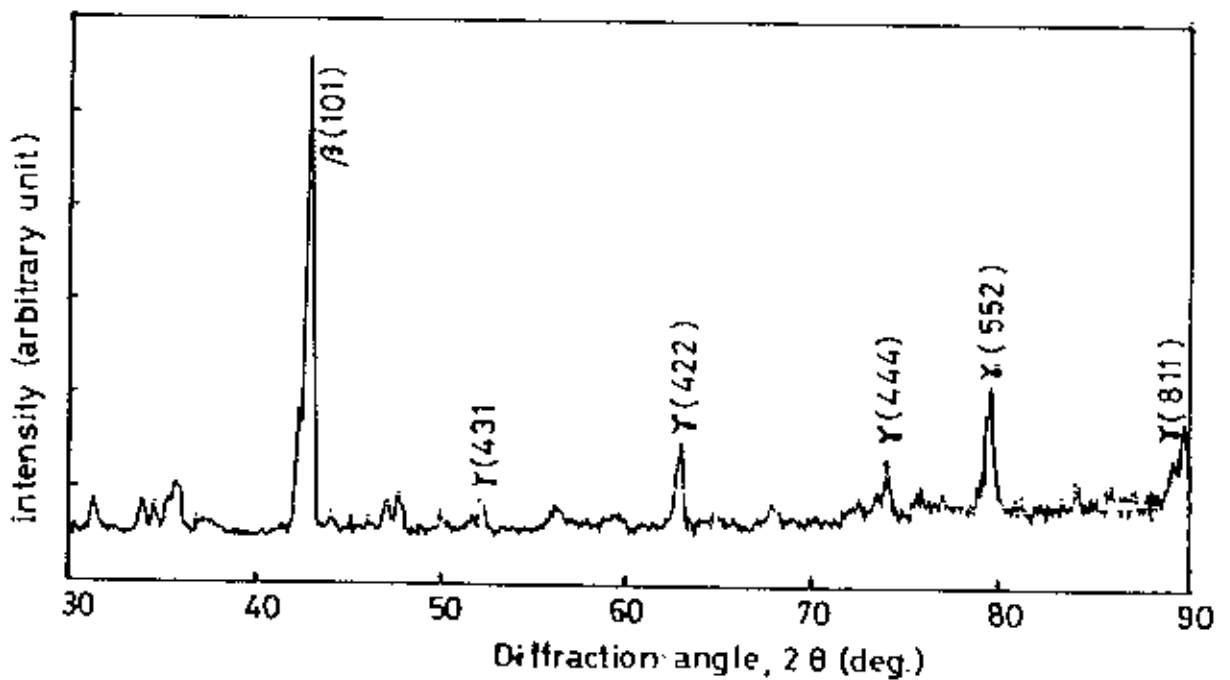


(b)

Fig.4.3: X-ray diffraction pattern of (a) as-deposited (b) annealed Zn-14.4% Ni alloy coating. (Deposition current density: 100 mA/cm^2 , Deposition time: 1 hr.)



(a)

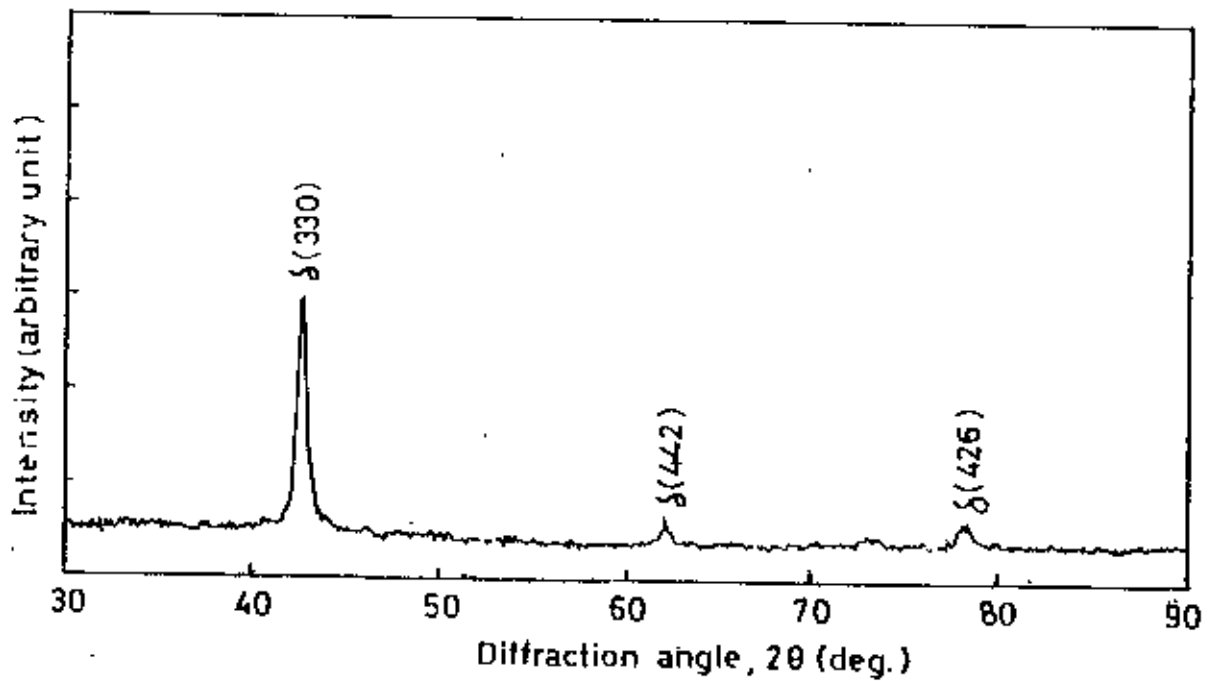


(b)

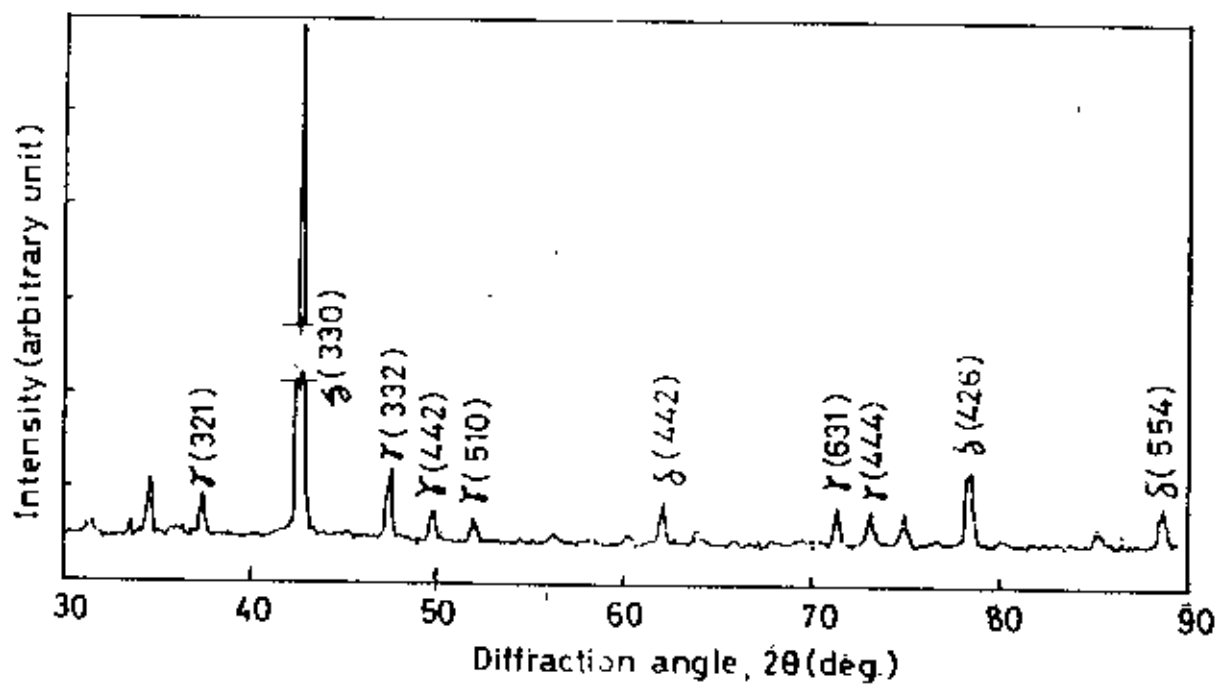
Fig.4.4: X-ray diffraction pattern of (a) as-deposited (b) annealed Zn-40%Ni alloy coating. (Deposition current density: 100 mA/cm^2 , Deposition time: 1 hr.)

Zn-7% Ni composition of Zn-Ni phase diagram lies in a two phase region of ($\delta+\eta$). Three diffraction peaks corresponding to (330), (442) and (426) planes of δ phase were detected in the as-deposited sample and peak of no η -phase could be detected. On the other hand, the annealed sample revealed some extra peaks representing γ and δ -phase and two unknown extra peaks. Both the patterns of as-deposited and annealed samples did not coincide with the Zn-Ni equilibrium phase diagram. The annealing was repeated and X-ray diffraction was taken again with a view to get new information to solve the contradiction. Yet the repeated X-ray pattern was the duplicate copy of the previous pattern of annealed sample. The reason for this contradiction could not be solved. Both the diffraction patterns are shown in Fig. 4.5.

Fig. 4.6 represents six diffraction peaks of η phase for the sample of as-deposited pure zinc coating. The peaks correspond to the plane (100), (101), (102), (103), (112) and (201).



(a)



(b)

Fig.4.5: X-ray diffraction pattern of (a) as-deposited (b) annealed Zn-7%Ni alloy coating. (Deposition current density: 100 mA/cm^2 , Deposition time: 1 hr.)

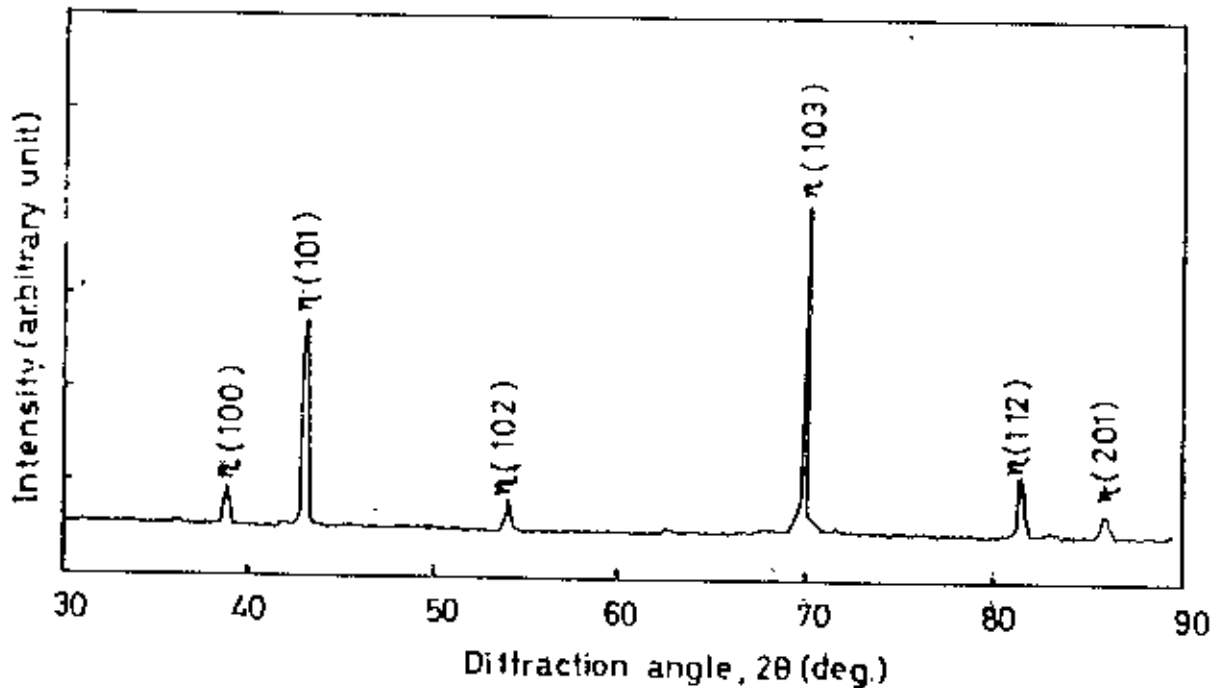


Fig.4.6: X-ray diffraction pattern of as-deposited pure zinc coating. (Deposition current density: 100 mA/cm², Deposition time: 1 hr.)

4.3 Microhardness Measurements

The microhardness of pure zinc coating and Zn-Ni alloy coating are shown as a function of Ni-content of the deposit in Fig. 4.7. All the coatings were deposited at room temperature at constant current density of 100 mA/cm². The hardness increases with increase in Ni content. The hardness increases at a faster rate at lower percentage of nickel. The hardness practically levels off after 14.4%Ni. Fig. 4.8 shows the effect of current density on microhardness of the coating deposited from different baths. It is seen that microhardness is independent on current density in every case. As hardness is independent on current density, it can be suggested that alloy composition is not affected significantly by current density variations. This is supported by the work done by others [36].

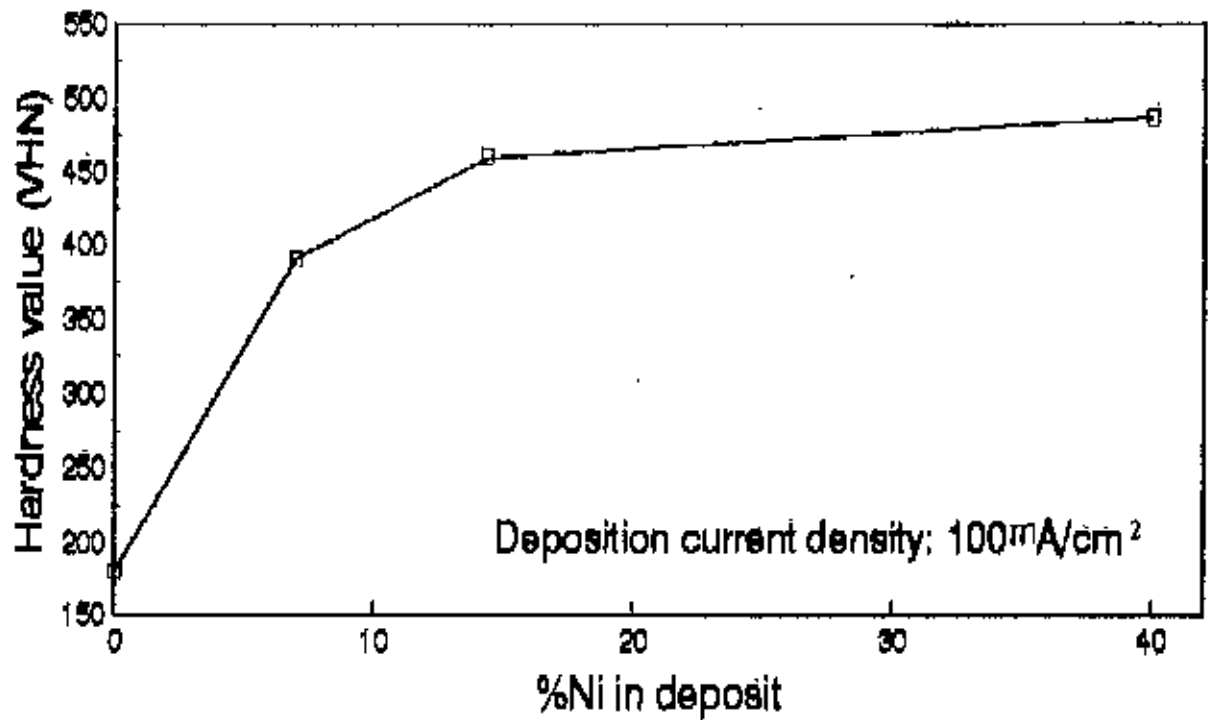


Fig.4.7: Effect of Ni content on microhardness

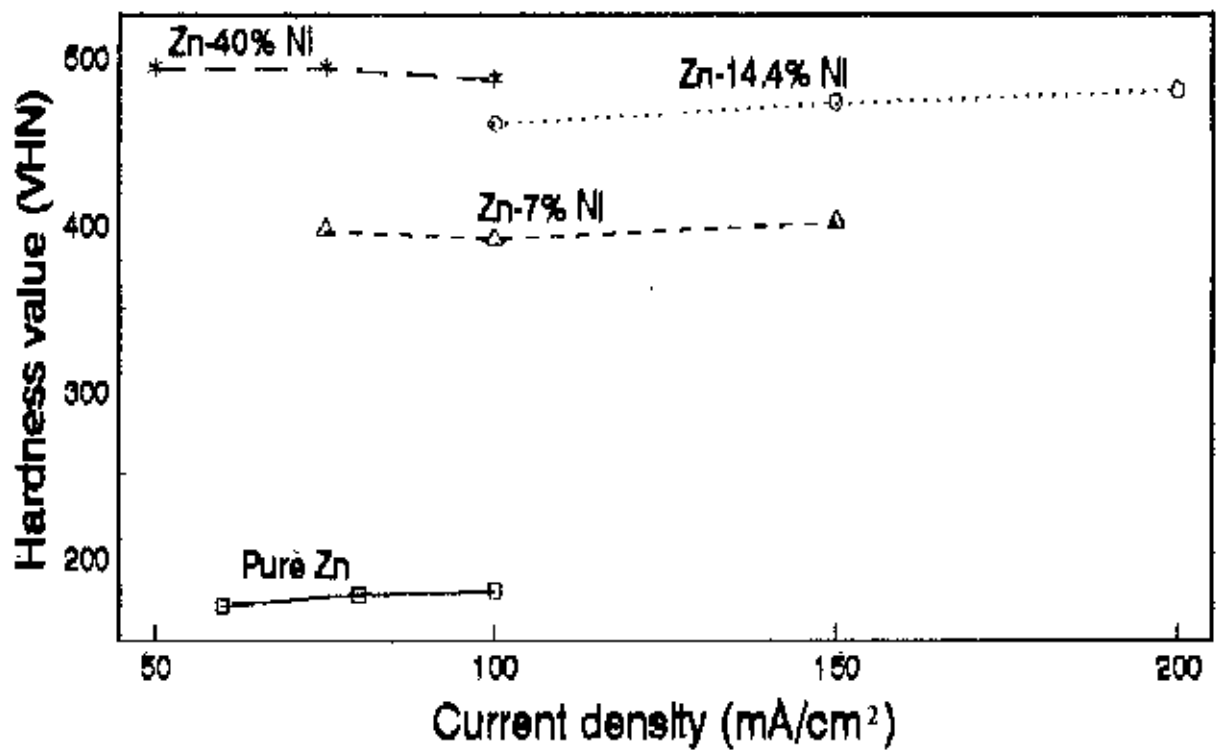


Fig.4.8: Effect of current density on microhardness

Fig. 4.9 shows a variation in hardness between as-deposited and annealed Zn-Ni alloy coatings of different composition. The hardness value of annealed deposit is a slightly lower than that of

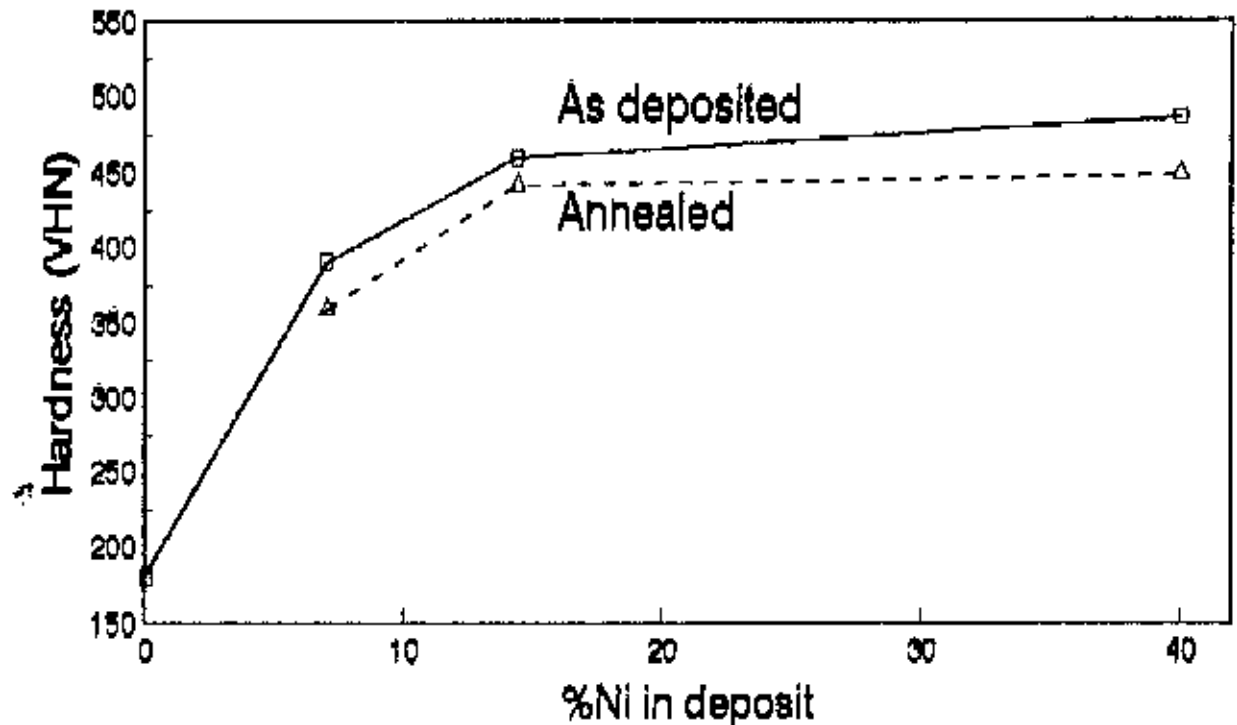


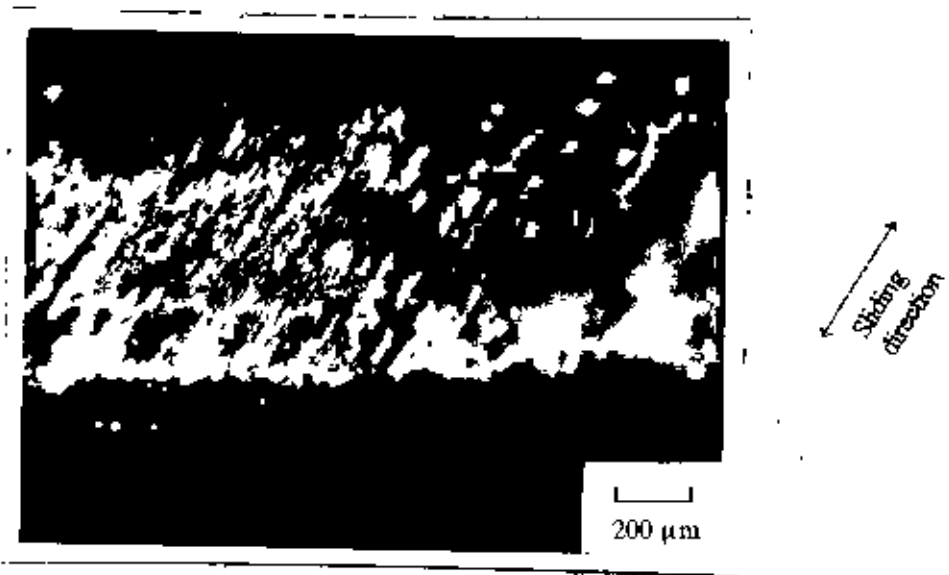
Fig.4.9: Variation in hardness between as-deposited and annealed Zn-Ni alloy coating

as-deposited coating. The as-deposited coating is believed to remain in a finely grained and stressed condition. Annealing of the coating causes the internal stress to be relieved and also results in grain growth [37]. Therefore lower hardness values are expected in annealed samples

4.4 Wear Test Evaluation

Fig. 4.10 shows the micrographs of wear scar on pure zinc, Zn-7%Ni, and Zn-14.4%Ni coatings tested under a load of 250 g for a sliding distance of 416 m. The micrographs were taken immediately after the test without any cleaning. It is seen that wear scar width is a function of deposit composition and the width increases with a decrease in nickel content of the

deposit. For pure zinc coating, the steel substrate was exposed which is seen as grey region at the middle of the wear scar [Fig. 4.10(a)].

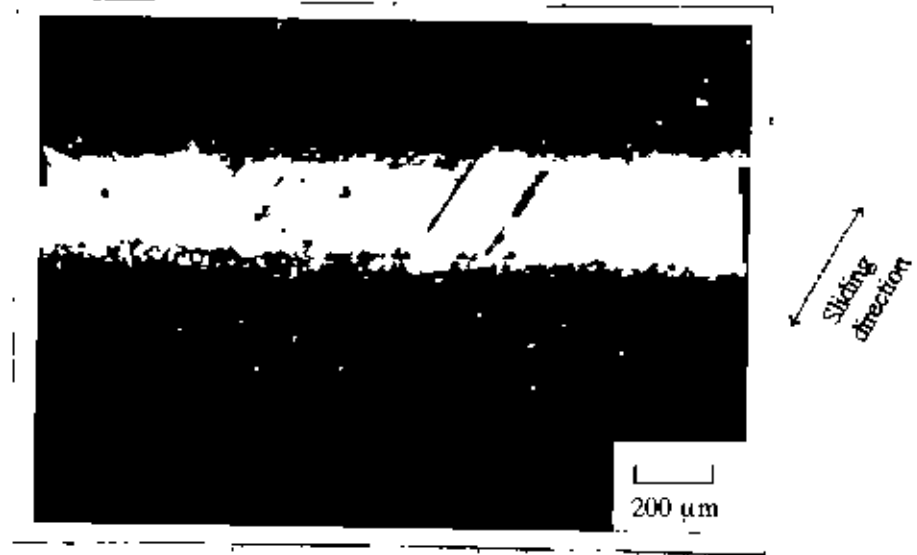


(a)

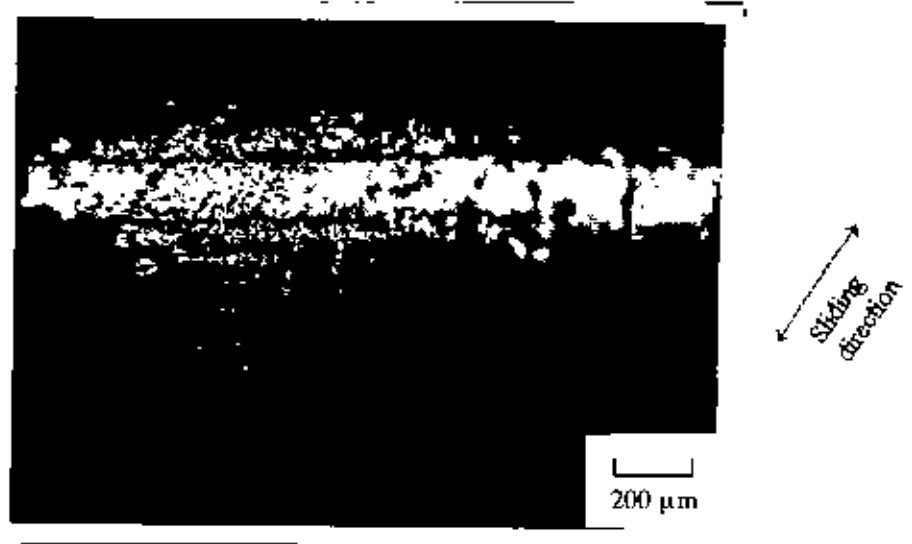
*Fig.4.10: Micrograph of wear scar of pure zinc coating
(Applied load: 250 g, Sliding distance: 416 m)*

In addition to some sliding marks, scar on pure zinc coating is found to be dirty. On the other hand, scars on Zn-7%Ni and Zn-14.4%Ni coating are seen to be smooth and clean. Fine sliding marks are also visible on both the micrographs of Zn-7%Ni [Fig.4.10(b)] and Zn-14.4%Ni [Fig.4.10(c)] coating.

Figs. 4.11-4.13 show the effect of sliding distance on wear scar width on the coated pin at various loads. From the figures, it is seen that Zn-Ni coating with 14.4% Ni is more wear resistant than the coating with 7% Ni. Pure Zn coating was tested for sliding distance of 416 m. Beyond this distance Zn coating totally disappeared and the substrate was exposed.



(b)



(c)

*Fig.4.10: Micrographs of wear scar of (b) Zn 7%Ni and (c) Zn-14.4% Ni coating
(Applied load: 250 g, Sliding distance: 416 m)*

Obviously pure zinc coating is found to be the least wear resistant. The rate of increase of the width of wear scar of both Zn-7%Ni and Zn-14.4%Ni alloy coating is seen to be higher at shorter sliding distance but the same tend to get reduced at higher sliding distance. The curves in Figs. 4.11-4.13 show this trend. With increasing sliding distance, this rate gradually decreases.

The wear rates of both zinc coating and Zn-Ni alloy coatings are shown as a function of load in Figs. 4.14-4.16. The anti-wear property increases with nickel percentage in the coating. The initial wear rate is high and gradually it becomes steady. The difference in wear rate between 14.4% Ni and 7% Ni for lower load (120 gm) is small but this difference increases with an increase in applied load.

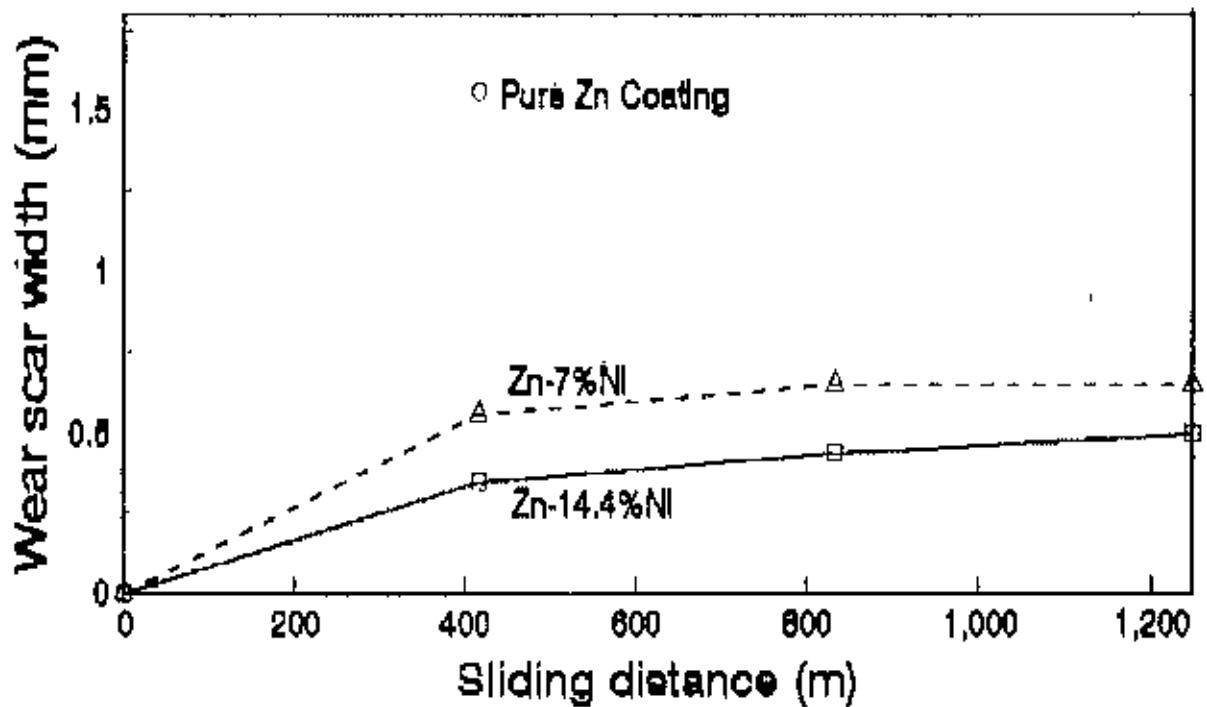


Fig.4.11: Variation of width of wear scar as a function of sliding distance at an applied load of 250-g.

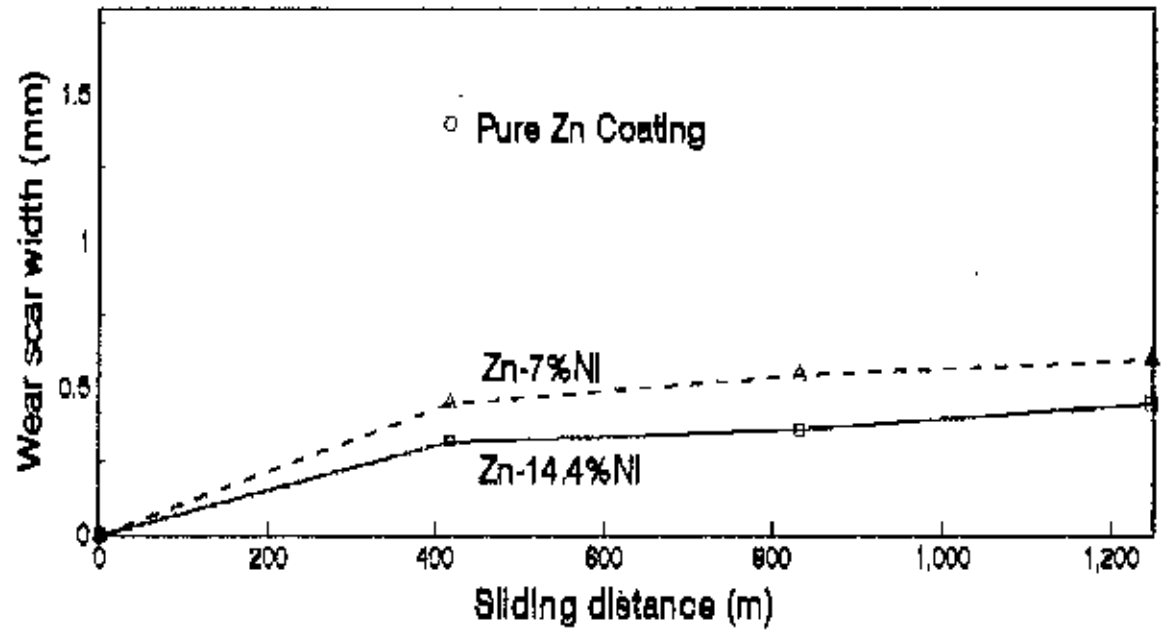


Fig.4.12: Variation of width of wear scar as a function of sliding distance at an applied load of 175 g.

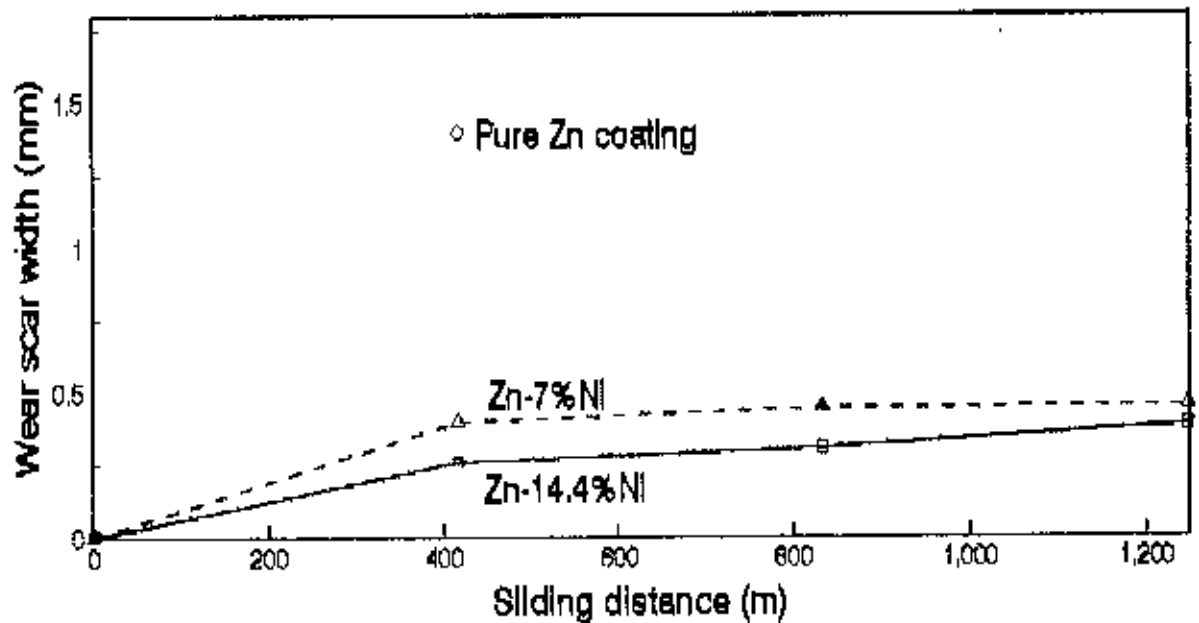


Fig.4.13: Variation of width of wear scar as a function of sliding distance at an applied load of 120 g.

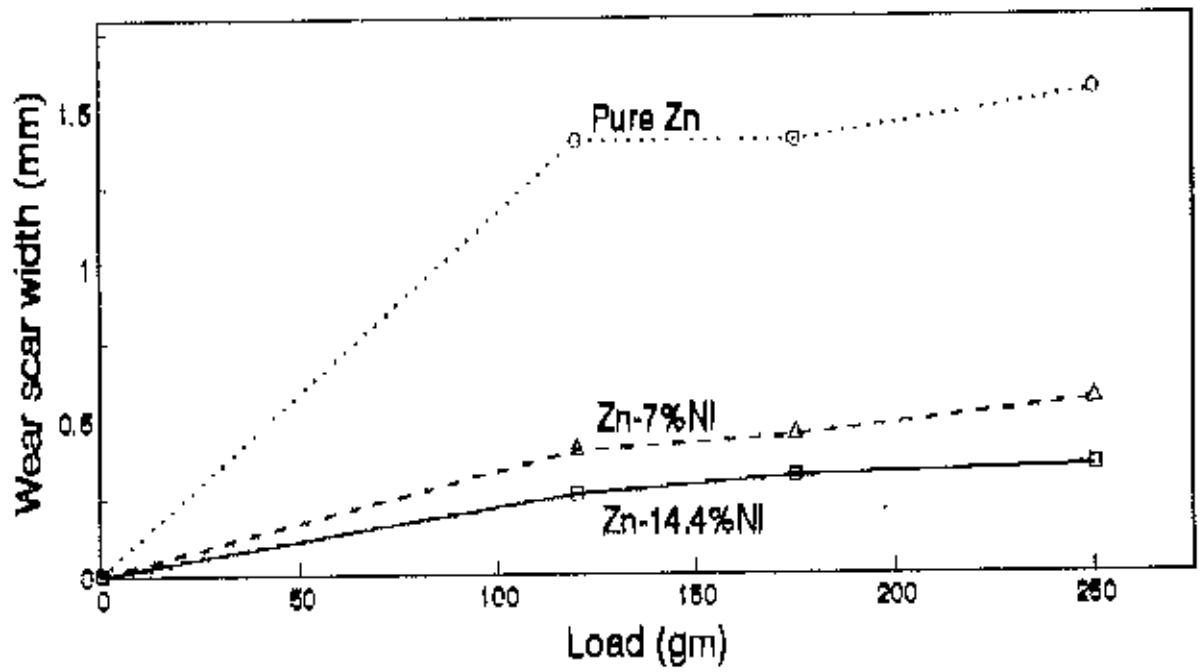


Fig.4.14: Wear scar width as a function of applied load (Sliding distance: 416 m)

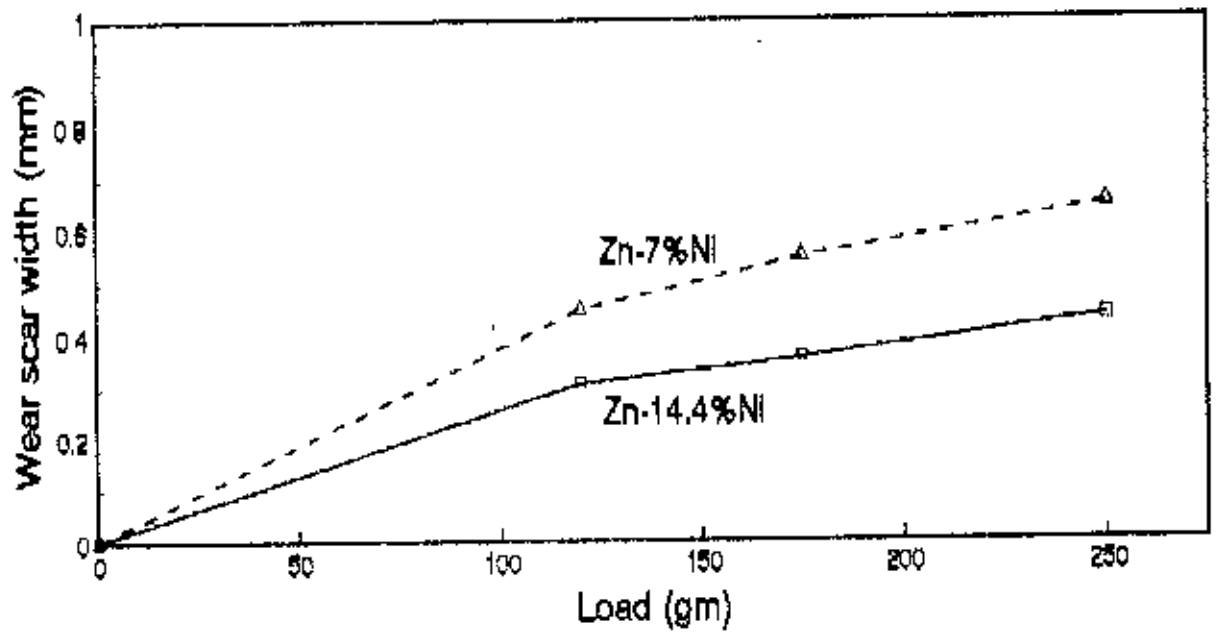


Fig.4.15: Wear scar width as a function of applied load (Sliding distance: 832 m)

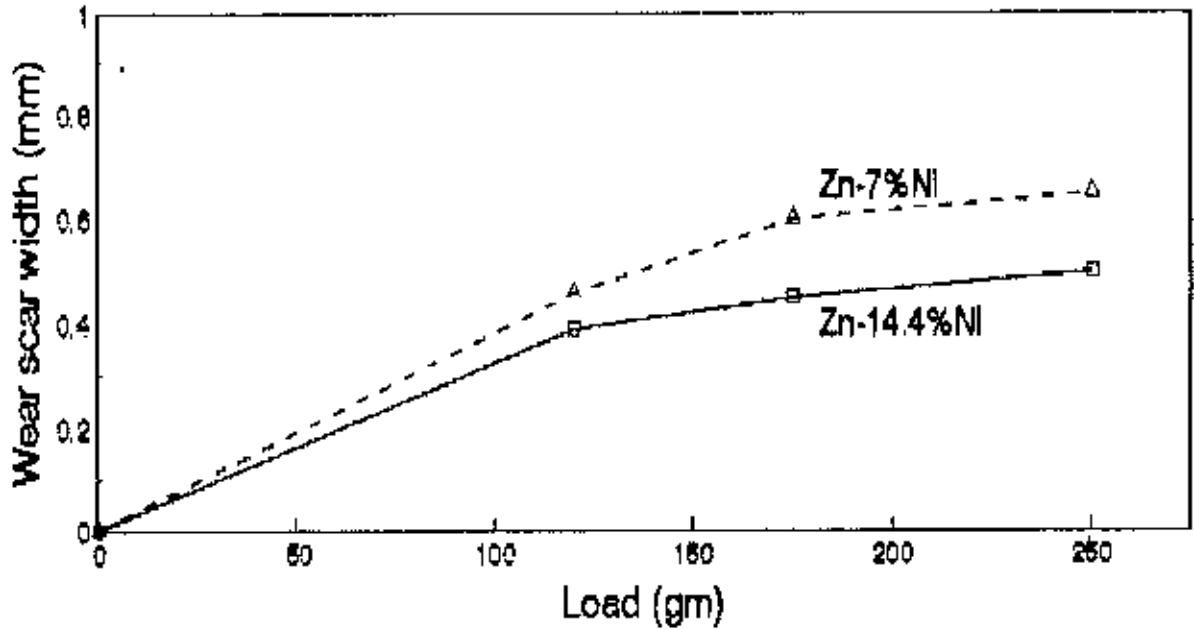


Fig.4.16: Wear scar width as a function of applied load (Sliding distance: 1248 m)

Fig. 4.17 shows the photomicrograph of wear scar on pure zinc coating tested for a sliding of 416 m. The micrograph was taken immediately after the test without any cleaning. In addition to some sliding marks, the worn surface is seen to mainly consists of dark areas containing attached debris or transfer layer. This suggests that adhesive wear is the main mechanism in the case of pure zinc coating

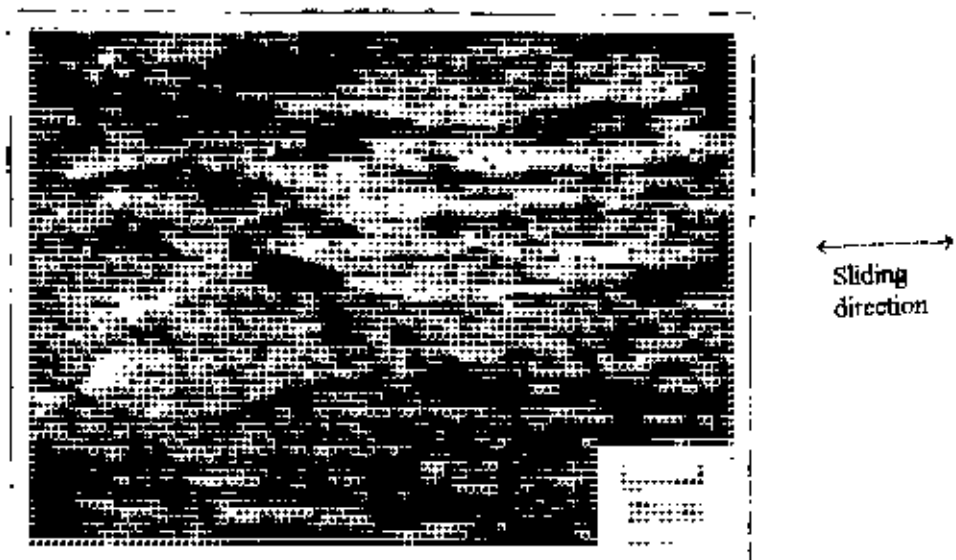
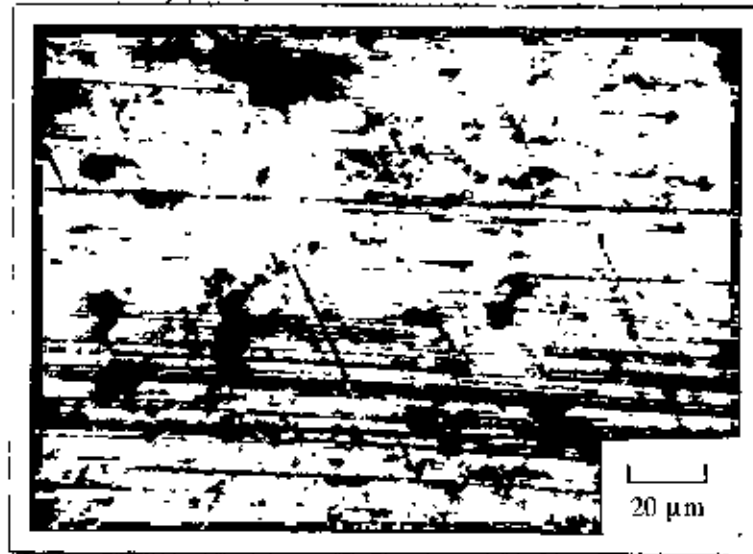


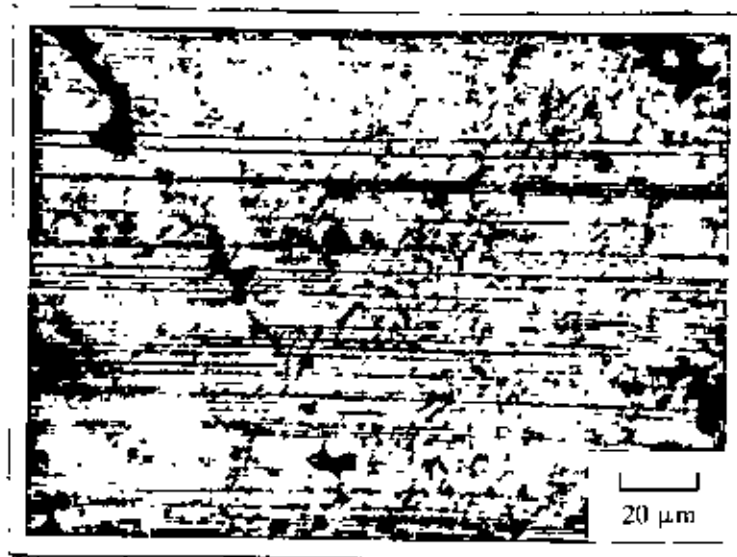
Fig.4.17: Micrograph of wear scar of pure zinc coating (Applied load: 250 g, Sliding distance: 416 m)

The micrographs of wear scars on Zn-7%Ni alloy coating is shown in Fig. 4.18. All the micrographs were taken without any cleaning of the scars. Scars on samples tested for 416 and 832 m are seen to be smooth and clean. Fine sliding marks is the main feature of these scars. On the other hand, scar on sample tested for 1248 m is found to be dirty. Patches of debris are seen to cling to the scar surface. The appearance of wear scar on Zn-7%Ni thus suggests that for distance upto 832 m, mainly abrasive wear operates. For longer sliding distance wear mechanism changes to the adhesive type. As an explanation, it can be said that heat is generated due to sliding for longer distance which creates a softening action on the alloy deposit. As hardness is decreased to some extent, adhesive wear tends to be dominant.

Like other type samples, the micrographs of Zn-14.4%Ni alloy coating were also taken immediately after the test without any cleaning of the scars. Fine unidirectional scratches on the microstructure are believed to cause the microcutting/ ploughing on the surface. Fine sliding marks is the main feature of the scars. Abrasive action of the fine debris also smoothens the scar. Thus abrasive wear is believed to be the main mechanism of Zn-14.4%Ni coating. Figs. 4.19 (a), 4.19 (b) and 4.19 (c) show the microstructure of wear scar for sliding distances of 416 m, 832 m and 1248 m respectively.

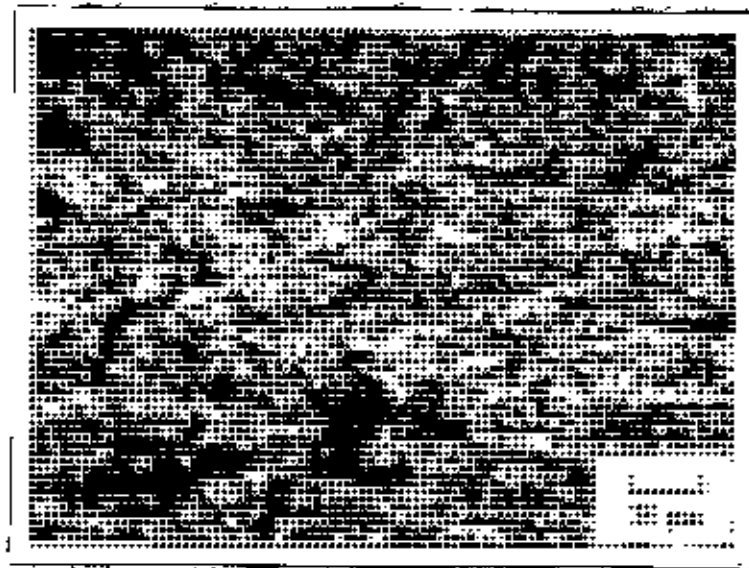


(a)



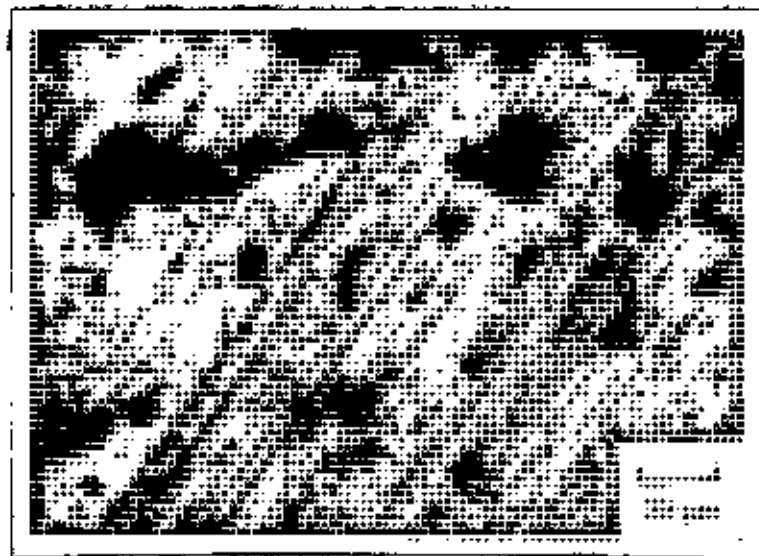
(b)

Fig.4.18: Micrographs of wear scar of Zn-7%Ni coating
(Applied load: 250 g, Sliding distance: (a) 416 m, (b) 832 m)



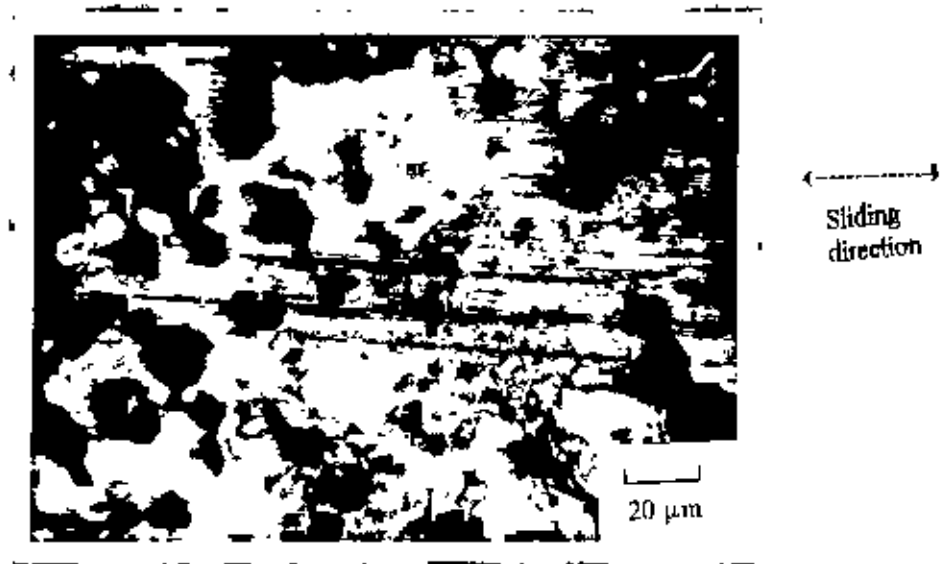
(c)

*Fig.4.18: Micrograph of wear scar of Zn-7%Ni coating
(Applied load: 250 g, Sliding distance: (c)1248 m)*

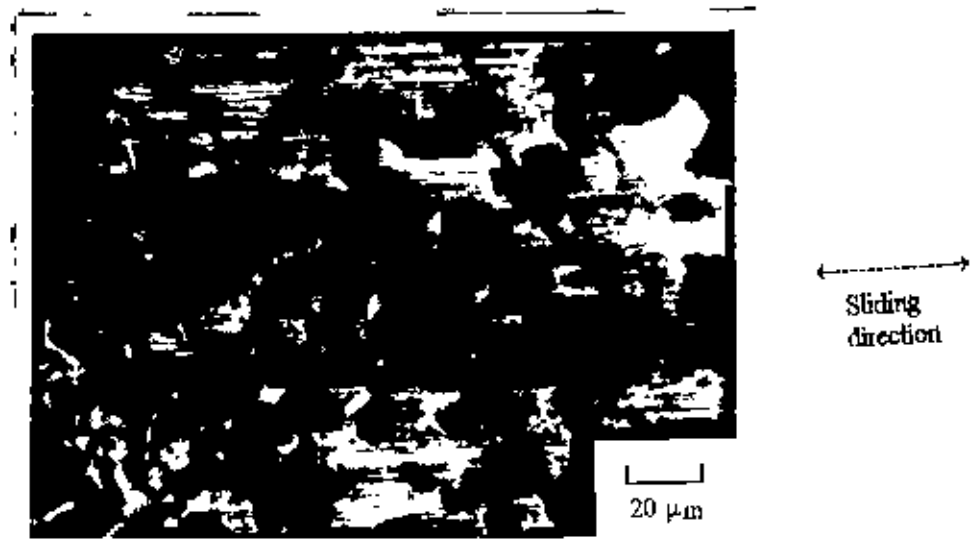


(a)

*Fig.4.19: Micrograph of wear scar of Zn-14.4%Ni coating
(Applied load: 250 g, Sliding distance: (a) 416 m)*



(b)



(c)

Fig.4.19: Micrographs of wear scar of Zn-14.4%Ni coating Applied load: 250 g, Sliding distance: (b) 832 m, (c) 1248 m

Islam et al. [38] have found that there is a relation between the hardness and wear rate of SG cast iron. The as-cast SG cast iron with low hardness value sustains more damage due to wear. The heat-treated SG cast iron with higher hardness value possesses higher wear resistance. The results of the present study also confirm to the above. Coating with 14.4% Ni, 7% Ni and 0% Ni are found to possess a hardness of 460 VHN, 390 VHN and 180 VHN respectively. Among the above three types of deposits wear rate of 0% Ni deposit is the highest and that of the 14.4% Ni deposit is the lowest. In Fig. 4.14, it can be seen that wear rate increases with a decrease in nickel content of the deposit. Fig. 4.7 illustrates that hardness decreases with decrease in nickel content of the deposit. The relation between hardness and wear resistance of the present zinc based coatings is seen in Fig. 4.20.

Sexton and Fischer [39] and Czichos [40] have found that the wear mechanism in steel depends upon its hardness. In martensitic steel with higher hardness, abrasive wear tends to take place. But for low hardness values, adhesive wear is encountered. The results of the present study also confirm to the above. For Zn-14.4% Ni alloy deposit with hardness value of 460 VHN, abrasive wear has been found to be the main mechanism while on the 0% Ni (100% Zn) metal coating with hardness value of 180 VHN, adhesive wear has taken place.

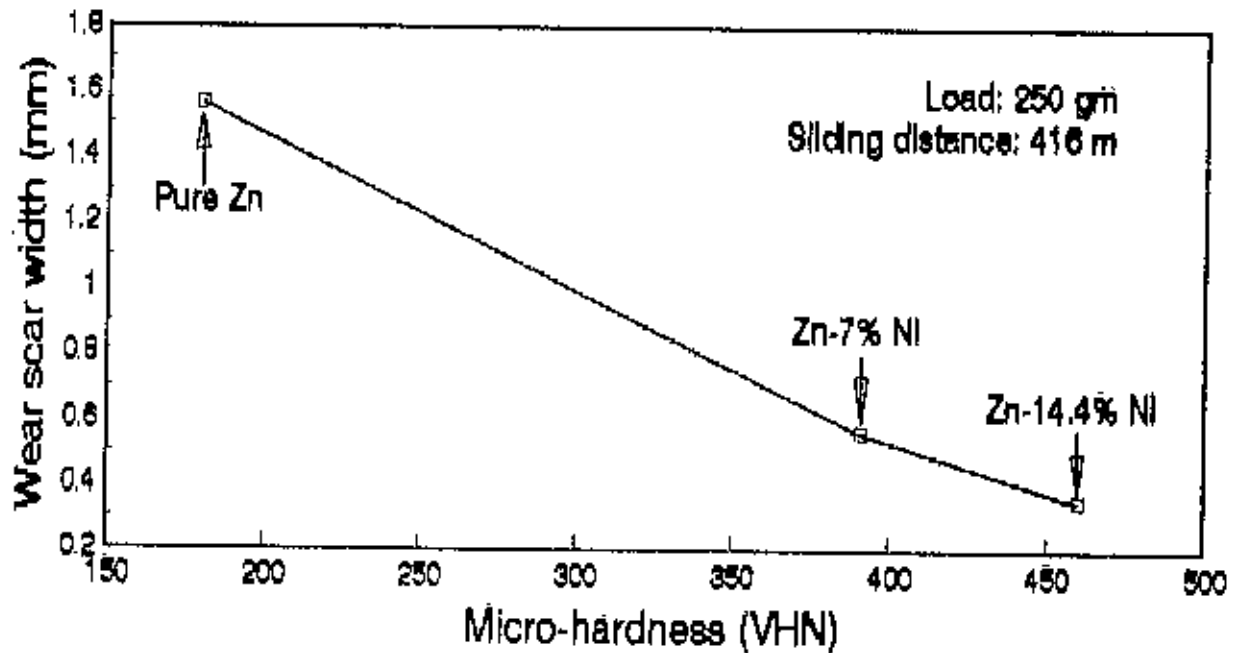


Fig.4.20: Effect of hardness on wear rate

4.5 Ductility Test

Coatings containing 14.4% Ni, 7% Ni and pure zinc coating were investigated for their ductility property. Every deposit was of 20 μ m thickness. As described in article 3.6.5, the present investigation involves a comparative study of ductility of different Zn-Ni alloy deposits with Ni-content. Pure zinc coating and coatings containing 7% and 14.4%Ni did not show any crack across or through it even at the smallest diameter (6 mm) mandrel. Therefore this method of bend test is not appropriate for comparing the ductility of zinc coating and Zn-Ni coating of varying nickel content. This test was not continued for coating with 40% nickel. An appropriate ductility measuring technique that can handle coatings with higher ductility should be used.

CHAPTER: FIVE

5. CONCLUSIONS**5.1 Conclusions Drawn from the Present Work.**

i) Uniform, adherent Zn-Ni alloy coatings may be deposited from a sulphate bath at room temperature and in the pH range of 1.8-3

ii) Deposition of Zn-Ni alloy is of anomalous type, where the less noble metal (zinc) deposits preferentially. There is a linear relationship between the %Ni in the deposit and that in the bath. Current density in the range of 50 to 200 mA/cm² is found to have no effect on %Ni in the deposit.

iii) Zn-40%Ni alloy and Zn-14.4%Ni alloy deposit with equilibrium phases.

iv) Both microhardness and wear resistance of coating increases with increase in nickel content of the deposit.

v) Wear of pure zinc coating having low hardness value is of adhesive type and that of Zn-14.4% Ni alloy coating having higher hardness value is of abrasive type. At lower sliding distance, abrasive wear is the main mechanism of Zn-7% Ni alloy coating while adhesive wear becomes predominant at higher sliding distance.

5.2 Suggestions for Further Work

- i) A further modification of electroplating process should be developed in order to get bright Zn-Ni alloy deposit without hampering the mechanical properties.
- ii) Ductility test methods other than ASTM B 489-68 bend test should be used to measure the ductility of Zn-Ni alloy coatings. Stretching test may be a useful method in this case.
- iii) Further research should be carried out to identify the unknown X-ray peaks of annealed samples and to find out the reason why the peaks did not appear in the as-deposited sample.
- iv) Further study should be carried out to confirm the occurrence of non-equilibrium phases in Zn-7%Ni alloy and find out the reason behind this.

REFERENCES

1. K. Ariga and K. Kanda, A Consideration on the Corrosion Resistance of Zinc-Cobalt based Co-electroplated Steel Sheet, *Tetsu to Hagane*, 66 (7), 1980, p.797.
2. J.W. Dini and H.R. Johnson, Electrodeposition of Zinc-Nickel Alloy Coating, Sandia Lab., 1977.
3. A. Shibuya, T. Kurimoto, K. Korekawa and K. Noji, Corrosion Resistance of Electroplated Nickel-Zinc Alloy Steel Sheet, *Tetsu to Hagane*, 66 (7), 1980, p. 771.
4. R.S. Bhakuni and S.K. Mowdood, Tires, The Goodyear Tire and Rubber Co., Akron, OH, 1987.
5. W.J. Van Ooij, *Rubber chem. Technol.*, 57 (1984), p. 421.
6. Y. Ishikawa and S. Kawakami, *Rubber Chem. Technol.*, 59 (1986), p. 1.
7. W.J. Van Ooij, Pirelli coordinamento Pneumatici S.P.A , Milan, Italy, Eur. Patent EP 0 283 738, September 28, 1988
8. R.S. Bhakuni and S.K. Mowdood, Tires, The Goodyear Tire and Rubber Co., Akron, OH, 1987.

9. A. Brenner, The Electrodeposition of Copper-Bismuth Alloys from a Perchlorate Bath, Ph. D. Thesis, University of Maryland, 1939.
10. S.G. Clarke, W.N. Bradshaw and E.E. Longhurst, Studies on Brass Plating, Electrodepositors' Tech. Soc., 19 (1994), p. 63.
11. F. Jepson, S. Meecham and F.W. Salt, The Electrodeposition of Iron-Zinc Alloys, Trans. Inst. Metal Finishing, 32 (1955), p. 160.
12. C.B.F. Young and C. Struyk, Deposition of Ni-Co Alloys from Chloride solutions, Trans. Electrochem. Soc., 89 (1946), p. 383.
13. E.P. Schoch and A. Hirsch, The Electrolytic Deposition of Ni-Zn Alloys, II. Trans. Am. Electrochem. Soc., 11 (1907), p. 135.
14. S. Glasstone and J.C. Speakman, The Electrodeposition of Co-Ni alloys, I. Trans. Faraday Soc., 26 (1930), p. 565.
15. C.G. Fink and K.H. Lah, The deposition of Ni-Co alloys, Trans. Am. Electrochem. Soc., 58 (1930), p. 373.
16. S. Glasstone and T.E. Symes, The Electrodeposition of Fe-Ni alloys, I. Trans. Faraday Soc., 23 (1927), p. 213.
17. E. Raub, Der Einfluss von Zusätzen Zu Nickelbädern auf die Schädlichkeit des Eisens. Mitt. Forschungsinst. U. Probieramts Edelmetalle staatl. höheren Fachschule Schwab. Gmund 9 (1935), p. 1-8.

18. W. Von Escher, A. Tenne, F. Herrschel and M. Schade, Über Passivitäts- und Verzögerungserscheinungen bei anodischer Entladung der Halogenionen und bei kathodischer Entladung der Ionen der Eisenmetalle, *Z. Elektrochem.*, 22 (1916), p. 85.
19. B. Lustman, Study of the Deposition Potentials and Microstructures of Electrodeposited Zn-Ni Alloys *Trans Electrochem. Soc.*, 84 (1943), p. 363.
20. E. Raub, Silber-Blei-Legierungen als Gleitlagerwerkstoffe, *Z. Metallk.*, 40 (1949), p. 170.
21. Ye Xingpu, Ph.D. Thesis, Faculty of Engg., Katholieke University of Leuven, Belgium, 1990.
22. Annual Book of ASTM standards, American Society for Testing Materials, 1916 Race St., Philadelphia, 1979, Part 9, p. 311.
23. A.X. Carcel and C. Ferret, Effects of Ni-Content on the Corrosion and Economic Performance of Zn-Ni Alloy Coatings, *Progress in the Understanding and Prevention of Corrosion. Vol.1*, The Institute of Materials, UK, 1993, p. 315.
24. C.C. De Minjer and A. Brenner, Further Studies of Electroless Nickel Plating, 44 (1957), p. 1297.
25. A. Brenner, Electrodeposition of Alloys, 1 (1963), p. 77
26. R. Sharan and S. Narain, *An Introduction to Electro-Metallurgy*, 2nd. Ed., Standard Publishers, New Delhi, 1991.

27. Sidney H. Avner, Introduction to physical Metallurgy, 2nd. Ed., McGraw-Hill Book Company, Auckland, 1974.
28. Metal Finishing, Guide Book Dictionary, 85 (1A), Metals and Plastics Publications, Inc., One University Plaza Hackensack, N.J.,(1987).
29. M. Jalal Uddin, M.Sc. Engg. Thesis, Dept. of Metallurgical Engg , Bangladesh University of Engineering and Technology, Dhaka, 1994.
30. J. Giridhar and W.J. Van Ooij, 'Study of Zn-Ni and Zn-Co Alloy Coatings Electrodeposited on Steel Strips', Surface and Coating Technol , 52 (1992), p. 17.
31. E. Gregory and W.W. Stevenson, Chemical Analysis of Metals and Alloys, Blackie and Son Limited, London, 1947, p. 230.
32. Metals Handbook, Vol.8, American Society for Metals, Metals Park, Ohio 44073, p.326.
33. R.H. Parker, An Introduction to Chemical Metallurgy, Pergamon Press, Oxford, 1967, p. 348.
34. A.J. Arvia and D. Posadas, in Encyclopedia of Electrochemistry of the Elements, A. J. Bard. Editor, Marcel Dekker Inc., New York (1995), p. 300.
35. D.E. Hall, Plat. Surf. Finish, 70 (1983), p. 59.
36. R. Albalat, E. Gomez, C. Muller, M. Sarret, E. Valles, 'Electrodeposition of Zinc-Nickel Alloy Coatings', Journal of Applied Electrochem., 20 (1990), p. 635.

37. B.E. Warren and B.L. Averbach, *Journal of Applied Physics*, 20 (1949), p. 885.
38. M.A. Islam, A.S.M.A. Haseeb and A.S.W. Kuny, *Study of Wear of As-cast and Heat-treated Spheroidal Graphite Cast Iron Under Dry Sliding Conditions*, Proceedings of the First Annual Paper Meet. BIT, Khulna, 1994, p. 38
39. M.D. Sexton and T.E. Fischer, *Wear*, 96 (1984), p. 17.
40. H. Czichos, in *New Direction of Lubrication, Materials, Wear and Surface Interaction in Tribology in the 80's*, N.R. Loonis (ed), Noyes Publication, NJ (1989).

APPENDIX: A

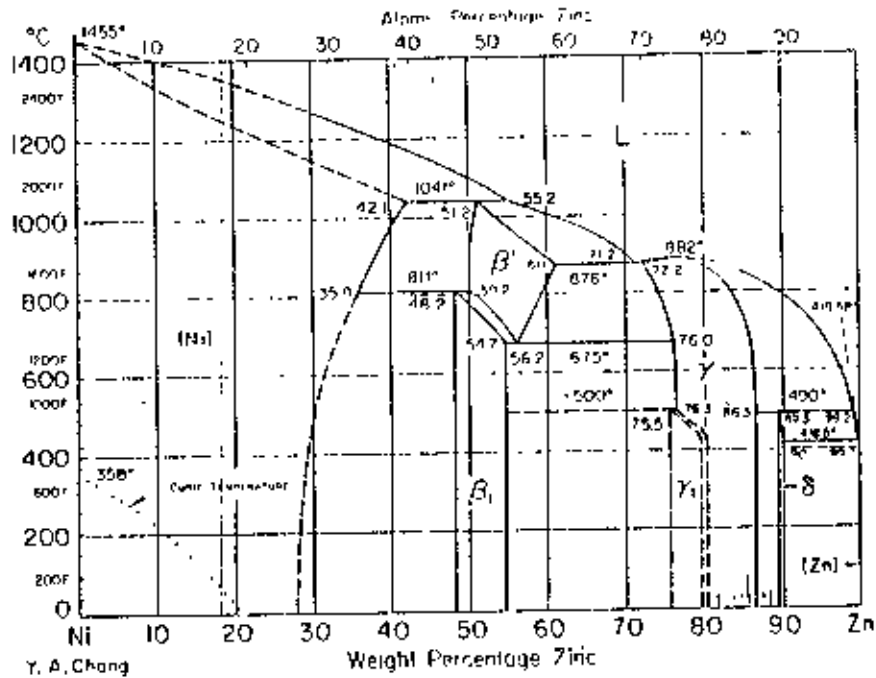


Fig.: Zn-Ni binary phase diagram [32]

(δ : Ni₃Zn₂₂, γ : Ni₅Zn₂₁, B^1 : BNiZn(HT), B_1 : B₁NiZn(LT), η : Zn)

